T.R.
BOLU ABANT İZZET BAYSAL UNIVERSITY
INSTITUTE OF GRADUATE STUDIES
Department of Physics

INVESTIGATION OF STRUCTURAL AND DIELECTRIC PROPERTIES OF ZNO NANORODS GROWTH BY HYDROTHERMAL METHOD

MASTER OF SCIENCE

AFRAH ABDULAZEEZ A.AL-KHAFAJI

ACADEMIC SUPERVISOR
Assoc. Prof. Dr. Sevgi POLAT ALTINTAŞ

BOLU, TEMMUZ - 2022

APPROVAL OF THE THESIS

Investigation of structural and dielectric properties of ZnO nanorods growth by hydrothermal method submitted by **Afrah Abdulazeez A. Al-KHAFAJI** and defended before the below named jury in partial fulfillment of the requirements for the degree of **Master of Science** in **Department of Physics, Institute of Graduate Studies of Bolu Abant Izzet Baysal University in 6.07.2022.**

Examining Committee Members	**Signature**
Supervisor Assoc. Prof. Dr. Sevgi POLAT ALTINTAŞ Bolu Abant İzzet Baysal University	....
Member Prof. Dr. Cihan PARLAK Bolu Abant İzzet Baysal University	....
Member Assoc. Prof. Dr. Ersin ORHAN Düzce University	....

Prof. Dr. İbrahim KÜRTÜL

Director of Institute of Graduate Studies

ETHICAL DECLARATION

In this thesis dissertation that was properly prepared according to the Thesis Writing Rules of Bolu Abant İzzet Baysal University of the Institute of Graduates Studies, I hereby declare that;

- All data, information, and documents presented in the thesis were obtained in accordance with the academic and ethical rules,
- All data, documents, assessments, and results were presented in accordance with the scientific ethical and moral rules,
- All works that were benefitted in the thesis were appropriately cited,
- No alteration was made in the data used,
- Study presented in this thesis is original,

Otherwise, I declare that I accept the loss of all my rights in case any contradiction that may arise against me.

Based on the plagiarisim report that was generated on the date of 6/06/2022 by using predertermined filtrations set by the Directorate of Insistute of Graduate Studies of the Turnitin programme, a plagiarism detection software, the rate of plagiarism detected was 27%.

AFRAH AL-KHAFAJI

ABSTRACT

INVESTIGATION OF STRUCTURAL AND DIELECTRIC PROPERTIES OF ZNO NANORODS GROWTH BY HYDROTHERMAL METHOD
MSC THESIS
AFRAH ABDULAZEEZ A. AL - KHAFAJI
BOLU ABANT IZZET BAYSAL UNIVERSITY
INSTITUTE OF GRADUATE STUDIES
DEPARTMENT OF PHYSICS
(SUPERVISOR: ASSOC. PROF. DR. SEVGİ POLAT ALTINTAŞ)
BOLU, JULY 2022
(XIII + 42)

Zinc oxide (ZnO) nanostructures is a significant material for optoelectronic and sensor devices due to the increasing demand for small-size fabrication of electronic devices in the industry. This thesis is an in-depth investigation of growth and physical properties of the ZnO nanorods (NRs) grown on glass and p-Si substrates. The structural properties and frequency-dependent dielectric function of the In/ZnO/p-Si heterostructures are also investigated. The NRs were produced by hydrothermal method on the substrates in a Teflon-lined stainless-steel cover at 90°C. Scanning electron microscopy analysis indicates nanorod morphology while LeBail refinement of XRD data showed that the ZnO NRs crystallize in hexagonal wurtzile structure with (002) orientation (space group $P6_3mc$). The dielectric properties of the In/ZnO/p-Si heterostructure were calculated with the help of experimental admittance measurements performed in the ±5 V voltage range and 1 kHz/1 MHz frequency range under ambient conditions. The real part of the complex relative permittivity (ε′), the imaginary part of complex relative permittivity (ε″) and loss tangent (tanδ) were obtained. Also, real (M′) and imaginary (M″) parts of the complex electric modulus (M*) were extracted. Frequency dependence in the ε′, ε″ and tanδ was attributed to the frequency dependence of the space charge polarization. The real part of electrical modulus was found to be nearly independent of frequency and voltage for positive voltages.

KEYWORDS: ZnO, Hydrothermal Method, Nanorod, Wurtzite,

ÖZET

HİDROTERMAL YÖNTEMLE BÜYÜTÜLEN ZNO NANOÇUBUKLARIN YAPISAL VE DİELEKTRİKSEL ÖZELLİKLERİNİN İNCELENMESİ
YÜKSEK LİSANS TEZİ
AFRAH ABDULAZEEZ A. AL- KHAFAJI
BOLU ABANT İZZET BAYSAL ÜNİVERSİTESİ
LİSANS ÜSTÜ EĞİTİM ENSTİTÜSÜ
FİZİK ANABİLİM DALI
(TEZ DANIŞMANI: DOÇ. DR. SEVGİ POLAT ALTINTAŞ)
BOLU, TEMMUZ - 2022
(XIII, 42)

Çinko oksit (ZnO) nanoyapıları, endüstride elektronik cihazların küçük boyutlu imalatına yönelik artan talep nedeniyle optoelektronik ve sensör cihazları için oldukça önemli bir malzemedir. Bu tez, cam ve p-Si altlıklar üzerine büyütülen ZnO nanoçubuklarının (NÇ'lar) büyütülmesinin ve fiziksel özelliklerinin derinlemesine araştırılmasıdır. In/ZnO/p-Si heteroyapılarının yapısal özellikleri ve frekansa bağlı dielektrik fonksiyonu da araştırılmıştır. NÇ'lar, 90°C'de bir Teflon astarlı paslanmaz çelik kap içinde altlıklar üzerinde hidrotermal yöntemle üretilmiştir. Taramalı elektron mikroskobu analizi, nanoçubuk morfolojisini gösterirken, XRD verilerinin LeBail iyileştirmesi, ZnO NÇ'larin (002) yönelimli (uzay grubu $P6_3mc$) altıgen wurtzile yapısında kristalleştiğini gösterdi. In/ZnO/p-Si heteroyapısının dielektrik özellikleri, ±5 V voltaj aralığında ve 1 kHz/1 MHz frekans aralığında gerçekleştirilen uygun ortam koşullarında ve deneysel kabul ölçümleriyle hesaplanmıştır. Bu hesaplamalardan karmaşık bağıl geçirgenliğin reel kısmı (ε′), karmaşık bağıl geçirgenliğin sanal kısmı (ε″) ve kayıp tanjantı (tanδ) elde edildi. Ayrıca, karmaşık elektrik modülünün (M*) gerçek (M') ve sanal (M'') kısımları ortaya çıkarıldı. ε′, ε″ ve tanδ'deki frekans bağımlılığı, uzay yükü polarizasyonunun frekans bağımlılığına bağlandı. Elektrik modülünün gerçek kısmının, pozitif voltajlar için frekans ve voltajdan neredeyse bağımsız olduğu tespit edildi.

ANAHTAR KELİMELER: ZnO, Hidrotermal Yöntem, Nanoçubuk, Wurtzite

TABLE OF CONTENTS

LIST OF FIGURES

Page

LIST OF TABLES

Page

LIST OF PICTURES

Page

LIST OF ABBREVIATIONS AND SYMBOLS

C	**:** Capacitance
D	: Deionized water
ε'	: Real part Dielectric
ε''	: Imagine part Dielectric
FT-IR	: Fourier Transform Infrared
G	: Conductivity
HF	: Hydrofluoric acid
HMTA	: Hexamethylenetetramine
MIA	: Monoethanolamine
M*	: Electrical Modulus
M'	: Real of the Electric Modulus
M''	: imaginary of the Electric Modulus
N_2	: Nitrogen gas
SEM	: Scanning Electron Microscope
tanδ	: Dielectric Loss Tanget
XRD	: X-Ray Diffraction
ZnO	: Zinc Oxide

ACKNOWLEDGEMENTS

I thank God Almighty first and foremost for the great blessing bestowed upon me, and I especially thank the distinguish to my supervisor Assoc. Prof. Dr. Sevgi Polat Altıntaş for helping me support me and guide me with advice, education, correction and all that she has done with me**.** I would also like to thank Dr. Nevin Soylu Koç for that spared no effort in help me, thank you very much to Dr. M. Gokcen and Dr. C. Altug for everything you gave me and helped me with scientific and laboratory information .

I would like to thank Dr. A. Varilci for assistance with laboratory measurements.

With many thanks to prof Dr. Cihan PARLAK and Assoc. Prof. Dr. Ersin ORHAN for them contributions and participation.

Then I would like to extend my thanks to those whose grace does not cease from me, my family will never stop all their efforts and their continuous support for me to these blessed moments.

1. INTRODUCTION

Nanotechnology, which uses nanoscale technologies to operate materials and devices, is now used in a variety of sectors of science. Nanoparticles are classed according to their diameter, which ranges from 1 to 100 nanometers (1).

Nanoparticles have recently gained a lot of attention, and because of their numerous electrical, magnetic, and optical properties, they are now considered one of the most widely employed materials in the development of many implementations. They're used in a variety of applications, including communications, sensors, transportation, optics, cosmetics, pharmaceuticals, industry, dye, medicine, biology, and the environment. ZnO is a new material with applications in many areas of life. It is used in gas sensors, chemical sensors, nano-sensors, beauty products, storage, optoelectronic devices, solar cells, and drug development. (2).

One-dimensional (1D), two-dimensional (2D), and three-dimensional (3D) structures of ZnO can be found. One-dimensional structures such as nanorods, nanowire, and ZnO can be obtained in two-dimensional structures such as the nanosheet and example of three-dimensional structures of zinc oxide is flower, one-dimensional particles such as nanorods attract a lot of attention due to their ability to use the building blocks of the electronic, photonic, and electromechanical future and photovoltaic devices, one-dimensional particles such as nanorods attract a lot of attention due to their ability to use the building blocks of the electronic. (3).

Amorphous and polycrystalline nanomaterials, particularly nanorods, have been developed. RF and DC sputtering, chemical vapor deposition (CVD), pulsed laser deposition (PLD), vapor phase transfer (VPT), and thermal evaporation have all been reported as ways for fabricating single-crystal ZnO nanorods. These approaches, however, are deemed high-cost since they necessitate a large amount of expensive equipment, ideal operating conditions, and relatively high working temperatures. (4).

Hydrothermal methods are significant for a variety of reasons. For example, when successful growth of ZnO microstructures on a glass substrate was demonstrated, this method garnered a lot of attention from researchers. However, this method isn't necessary. Different nanoforms can be obtained easily by modifying the hydrothermal conditions. Sophisticated equipment for being low cost and environmentally benign, therefore ideal (5), Furthermore, because hydrothermal development takes place at very low temperatures, nanostructures can be formed on a wide range of substrates. (6).

1.1 History of ZnO

With the first application of ZnO for semiconductor qualities in the 1930s, there was a surge in interest in this material. Researchers concentrated on the growth and usage of ZnO after discovering its appealing semiconductor properties in the 1950s. ZnO thin films have the potential to be used in sensor and catalytic applications, the synthesis of ZnO thin films was widely researched in the 1960s. Since the 1990s, it was there a lot of interest in the synthesis of ZnO nanostructures utilizing various growth techniques, with hundreds of articles and patents being published every year since 2000. (7).

The present revival in ZnO research began in the mid-1990s, as evidenced by several conferences, seminars, and symposia, as well as more than 2000 ZnO-related publications published in 2005 and 2006, compared to just over 100 in 1970. (8). However, in the last ten years, interest in zinc oxide has increased, as nearly 70,000 papers have been published from 2007 to 2022.

Modern technology today relies on the development of superstructures, quantum wells, nanoarms and similar items, or quantum dots, in addition to or instead of GaN-based structures, as well as the prospect of getting a blue/ultraviolet optoelectronic material, such as light emission. Laser diodes are also used.

1.2 Definition of ZnO

Zinc oxide, commonly known as zincate, is an inorganic substance that is found in nature in crystalline form only very seldom. It's normally a white crystalline powder that's semi-insoluble in water, and the majority of ZnO utilized in commercial applications is made in a factory. Because of oxygen vacancies, the zinc oxide compound is an n-type wide bandgap semiconductor of group II-VI semiconductors. (9).

A white solid compound that yellows upon heating due to lattice distortions. Furthermore, unlike cadmium compounds, it is regarded a non-toxic material that is insoluble in water and alcohol but soluble in acetic acid, mineral acids, ammonia, and alkaline hydroxides. Therefore, it is an amphoteric oxide. Zinc oxide is prepared chemically from zinc salts as well as burning Zn in the air or by thermal cleavage of its carbonate or nitrate Picture (1.1) (10).

Picture 1.1 Zinc oxide powder

ZnO, like GaN, will be significant for blue and UV optical devices due to its wide bandgap of 3.4 eV and large exciton binding energy of 60 meV at ambient temperature. In this application, ZnO provides a number of benefits against GaN. The capacity to develop single crystal substrates and its higher exciton bonding energy are the most crucial. Other advantages of ZnO include its broad chemistry, which allows for a wide range of wet chemical drilling applications, a low energy threshold for optical pumping, and biocompatibility. These properties of ZnO combine to make it an excellent choice for a wide range of devices, including ultraviolet laser diode sensors and nanotechnology-based electronics like screens (11).

Table 1.1. ZnO's fundamental physical and chemical properties. (12).

Properties	Values
Molecular mass	81.37 g/mol
Temperature at which something melts	1975 °C
Temperature at which water begins to boil	sublimes
Solubility	0.16 mgram/100 mL water (30 °C)
Crystal structure that is stable	wurtzite
Parameters for the lattice	a = b: 0.32495 nm c: 0.50269 nm
The energy of the band gap	3.4 eV
Binding energy for exciton	60 eV
Density	5.606 g/cm^3
Rerractive index	2.008
Electron effective mass	0.24
Static dielectric constant	8.656

1.3 Interaction and Risk

Zinc oxide is a stable, non-flammable compound that does not show any incompatibility with other chemical compounds, but when heated, it emits toxic fumes, the compound is not toxic or dangerous when ingested or in contact with the skin or eyes, but it is better to wash them well when touching them, however the compound presents an inhalation hazard, a harmful concentration of particles in air can be reached quickly relative to zinc oxide particles. Inhalation of fumes can cause metallic smoke fever, also, studies have not proven its ability to cause cancer. (13). Although zinc oxide is used as a medicine, it is highly toxic to the environment, especially to aquatic organisms, however, the toxicological to zinc oxide varies between aquatic organisms according to nutritional levels (14).

1.4 Applications o ZnO

Zinc oxide is widely employed in a variety of applications, spanning from cosmetics to optoelectronic devices, medical areas, and general application fields, and its global consumption is estimated to be around 105 tons per year due to its unique features.

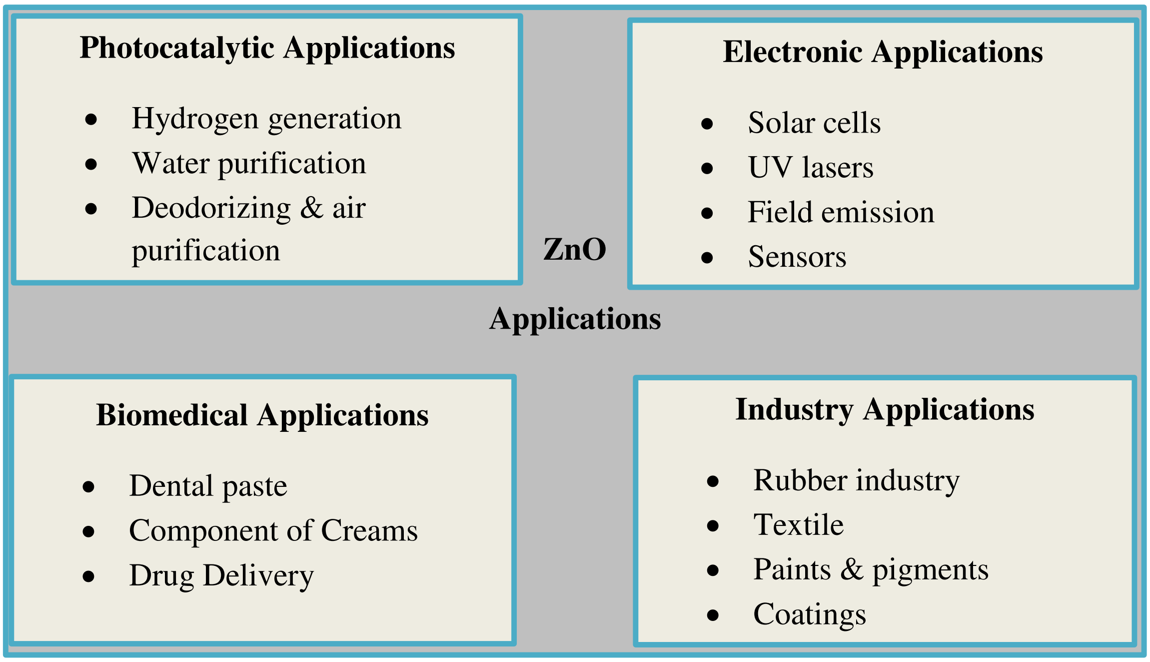

Figure 1.1. Applications of ZnO. (15).

1.5 Properties of ZnO

1.5.1 Chemical Properties of ZnO

There are two oxidation states for zinc: +1 and +2, with the latter being the more common, while there have recently been debates about the possibility of a third +3 oxidation state in the shape of bulk zinc oxide, which is moderately soluble in water under neutral conditions (-5 mg L^{-1}). Zinc oxide nanoparticles, on the other hand, have been shown to have increased water solubility at neutral pH levels, and numerous parameters like as size, crystal, and shape can influence dissolving rates. Zinc oxide nanoparticles have been found to exhibit solubility values of 718-740 mg L^{-1} in pure water at pH 7.3, and zinc oxide solubility was already confirmed at temperatures ranging from 150 to 350 degrees Celsius. (16).

1.5.2 Electrical Properties of ZnO

At ambient temperature, zinc oxide has a large band gap of 3.37 eV and a high exciton bonding energy of 60 meV. ZnO has a considerable light absorption in the UVA (315-400 nm) range, making it appropriate for applications, because of these advantages, by grafting impurities with metal cations, it is possible to significantly alter the structural, optical, and electrical properties of zinc oxide, which is a very valuable procedure for the production of various electrical and electronic devices, light emitting diodes. Quantitative confinement of charge carriers and electrical characteristics of ZnO derived from original point defects such as oxygen vacancies (V_o) and interstitial zinc (Zni^+). (17).

Doping is a simple approach for modifying the electrical, optical, magnetic, piezoelectric, and electronic properties of ZnO by varying the concentration of the original point defects and impurities (up to 10^{-14} cm^{-3} or 0.01 ppm).

1.6 DOPING of ZnO

1.6.1 Doping

When limited percentages of impurities are added to a semiconductor crystal, this process is called doping, and the number of impurities added is known as (Level Doping) and these impurities create new energy levels that fall into the gap banned between the conductivity and valence band.

Even in the absence of doping, most ZnO has an n-type nature; the majority of ZnO has an n-type character. Original flaws, for example it's commonly considered that oxygen vacancies or zinc interlayers are to blame. However, the issue is still up for debate. Based on the theory, an alternate explanation has been provided. Unintended replacement hydrogen contaminants are to fault in the computation can be manipulated, Zn can be easily replaced with the third group elements Al, Ga, and In, or oxygen can be replaced with the group VII elements chlorine or iodine to obtain n-type doping. ZnO p-type activators that are reliable it's still a challenge; the limited solubility of p-type and.-doping compounds causes this issue. Compensation is provided by a large number of n-type impurities, which applies not only to ZnO but also to other metals GaN and ZnSe (18).

1.6.2 N-Type Doping

For n-type doping Zn or O are replaced by atoms containing one more electron in the outer shell of the atom that it replaces, so the third group elements Al, Ga and In are s in a despite numerous researches, the properties of ZnO are still not as clear as nature's of the n-type residual conductivity in unblown ZnO films whether caused by impurities from an original defect or its flaws, as some researchers are still under research the remaining background is attributed to intrinsic defects in oxygen Vacancies V_o and interstitial zinc atoms Zni, or to uncontrollable hydrogen impurities that are introduced during growth, surface and active donors on zinc cation sites.

Group III elements like Aluminum and Gallium, along with group VII elements like Chlorine and Bromine, are examples of n-type dopants in ZnO (19).

1.6.3 P-Type Doping

Although progress has been made in obtaining p-type in ZnO films utilizing various growth processes and different impurities of group –V (N, P, As, and Sb), high-quality, reliable p-type conductivity of ZnO has yet to be obtained. Some basic properties of ZnO remain unknown, such as the nature of n-type residual conduction in unblown ZnO films, whether it is caused by impurities from an original defect or defects, and the remaining background is credited to inherently defects oxygen vacancies (V_o) and interstitial zinc atoms (Zni) and other it cannot be controlled hydrogen impurities introduced all through growth, according to some researchers. (20).

P-type doping in ZnO may be possible by substituting either group - III elements such as Li for Zn sites or Group-V elements such as N for O sites.

1.7 ZnO Structure

Zinc oxide can be found in one-dimensional, two-dimensional and three - dimensional structures and the structures are more one - dimensional than others.

The crystal structure of zinc oxide is of three types (Fig 1.1):

a - Wurtzite (hexagonal symmetry)

b - Zinc-blend

c - Rock salt

The zinc-blend cube can be made stable, when it is grown on cube-shaped bases as for the rock structure, it is obtained at ambient temperature and pressure by as for its structural construction, it consists of two overlapping parts that focus on the face A cubic grid consisting of various elements along the diagonals of the body corresponds to half the length of diameter. (21).

The wurtzite structure of ZnO crystals is more common and stable, and the crystal structure is similar to the group (VI-II) of semiconductors, which is a hexagonal lattice that corresponds to space with the group P63 mc. The hexagonal unit cell has lattice parameters of a = 3.2495 and c = 5.2069, and a density of 5.605 g cm3 (Figure1.2), with two interconnected subnets of Zn^{+2} and O^{+2}, with each Zn ion surrounded by a tetrahedron of O ions, and conversely. Polar symmetry along the hexagon axis is created by this tetrahedral coordination. It also has piezoelectricity and spontaneous polarization, and it is a crucial factor in crystal formation, drilling, and defect creation. (22).

ZnO with a wurtzite structure has two closely packed hexagonal overlapping sub-lattices which consist of one type of atom (Group II) surrounded by another type of atom (Group VI) along the triple c axis. (23).

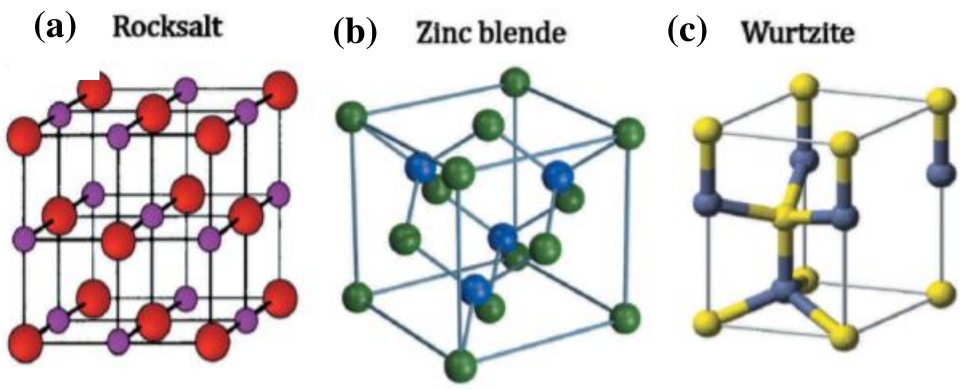

Figure1.2. Crystalline Zinc Oxide Characterization (a) Rock salt, (b) Zink blende, and (c) hexagonal Wurtzite respectively**.** (24)**.**

1.8 Synthesis of ZnO

Several approaches were used to make ZnO nanorods, like chemical vapor deposition, hydrothermal method, radio frequency sputtering, sol-gel method, vapor condensation method, spray pyrolysis, thermochemical techniques, pulsed laser deposition and other technologies. But among all the methods, the hydrothermal method is of great importance because of its many advantages. It is considered a simple technology and requires a low temperature that does not exceed 100 ºC, high productivity and ease of control greatly compared to the previous methods. (25).

1.8.1 Solid-State Reaction

Zinc oxide can be extracted directly from zinc ore (the American method) or indirectly from zinc ore (French process).

1.8.1.1 American Process

Reduction-oxidation processes are used in this production process, different from the French process, which uses pure zinc metal as a feedstock, the American process can use a range of materials that are intermediates such as those zinc-containing compounds and zinc mineral ores, which may contain several elements such as impurities, slag, furnace slag, or Zinc oxide is out of grade, the carbothermal reduction of the raw material to zinc metal is the first step in the American or direct synthesis process, this is accomplished by first heating the feedstock and then mixing it with a graphitic carbon source. the feed stock is reduced to zinc metal as a result of the CO_2 / CO mixture generated from the carbon source, which subsequently melts and vaporizes as the temperature rises, the zinc vapor is then sent into an oxidizing chamber, where it is converted to zinc oxide particles and collected in a manner similar to the French method. (26).

The resulting zinc oxide (direct method) impurities in the form of composites from different zinc ore minerals are present. The resulting zinc oxide particles are mainly needle-shaped, sometimes spherical.

1.8.1.2 French Process

Metallic zinc is melted in a furnace and vaporized at 910°C in this indirect method. ZnO is formed when zinc vapor reacts with oxygen from the air in an instantaneous reaction. The zinc oxide particles are collected in a bag filtration facility after passing through a cooling channel. In 1844, Le Claire pioneered the indirect method. Conglomerates with an average particle size of 0.1 to a few micrometers make up the product. The majority of the zinc oxide particles are spherical in form. Vertical furnaces are used in the French process. (27).

1.8.2 Sol – Gel Method

Sol-gel technology describes the process of converting a liquid solution to a rigid gel matrix. It is based on hydrolysis condensation and drying, which are both physical and chemical interactions.

The sol-gel method is widely used to fabricate ZnO nanostructures due to its reliability, simplicity and moderate synthesis conditions. (28).

The materials are syntheticd by solidifying a solution, sol, or gel containing a chemically active ingredient, and thereafter thermal treatment an oxide or other compound under moderate conditions.

Sol-gel technology has proven to be effective in the production of oxide coatings, glass, and ceramic powders, particularly compound oxide materials and superconductivity materials with threshold temperatures that are difficult to create using traditional methods.

ZnO because of their simple implementation, sol-gel nanoparticles are frequently employed. One of the benefits of sol-gel technology is the ability to use many precursors (29).

1.8.3 Hydrothermal Method

In this procedure, the mixture of substrates is progressively heated to a temperature of 100-300 ° C on a range of flexible/soft plastic and paper substrates and left for several days in an autoclave. The effect of heating is the formation of crystal nuclei, which then grow as a result of cooling. The ability to carry out the synthesis at low temperatures, the various shapes and dimensions of the resulting crystals, which are dependent on the chemical composition of the starting mixture, the high degree of crystallization of the result, as well as the procedure's temperature and pressure, and the material's high purity, are all aspects of this method. (30), also, one of the advantages of this technology low energy consumption, low cost and easy handling. (31).

1.8.4 RF Sputtering

Radio Frequency Spray Technology ZnO thin films made using RF sputtering have several advantages, including high purity, homogeneity, rough surface, and nanostructure characteristics. Two techniques can be used to make ZnO thin films in this technique. The use of a ready-made ZnO cathode is one of them. The other is zinc oxidation, which necessitates the use of a working gas such like Argon, as well as oxygen mixing in general. (32).

This technology is relatively flexible to achieve a high rate the sedimentation ratio ensures adherence to a wide range of materials while maintaining clear thin films' optical and electrical qualities. (33).

1.8.5 Precipitation Method

This is a common method for obtaining zinc oxide with repeatable characteristics. The method entails reducing a zinc salt solution with a reducing agent to limit the formation of particles of particular dimensions, then precipitating the ZnO predecessor from the solution, heat treatment, and grinding to eliminate impurities. Temperature, pH, and precipitation time all influence how much rain falls (34).

This technique it has many advantages, more controllable, it can be reproduced and the particle size obtained can be easily control (35).

1.8.6 Method Using an Emulsion

Emulsion is employed in a range of sectors as a precursor for the manufacture of solid polymer microparticles, solid lipid nanoparticles, inorganic nanoparticles, and oil-filled microcapsules, as well as magnetic particles for imaging and diagnostics.

An emulsion is a mixture of Two liquids that are not miscible with each other, oil in water (Oil/Water) and water in oil (Water/Oil). In this definition, any quite polar and hydrophilic liquid will drop into the water, while non-polar liquids are considered hydrophobic (oils) (36).

Emulsions and micro-emulsions are significantly different from one another, making it easier to distinguish between them. Micro-emulsions arise spontaneously under the right conditions.

When preparing zinc oxide using the emulsion method, when using the emulsion method to generate zinc oxide, zinc oleate (melted in decane) reacts with sodium hydroxide in an interphase reaction (dissolved in ethanol or water) (37), Temperature, substrates, and the two-phase component ratio are all factors to consider affects the particle size and location of these factors, which are the conditions for this process (38).

1.8.7 Spray Pyrolysis Method

Spray pyrolysis is an enhanced chemical vapor deposition approach for the fabrication of nanotubes. It was shown that nanotubes generated using spray pyrolysis had several unique properties when compared to nanotubes fabricated using traditional methods.

A reactor tube, furnace, and ultrasonic atomizer are used in the spray pyrolysis process. The reaction is carried out by heating the precursor solutions to temps that cause the solute to pyrolyze.

Because of its strong water solubility and low temperature of division, $Zn(CH_3COO)_2H_2O$ is utilized as a zinc precursor in the pyrolysis process to create zinc oxide particles. The breakdown of zinc acetate dihydrate is used to determine the mechanisms and dynamics of heat, as well as the relationship between the mechanism and the pyrolysis process results, this technique has several advantages, such as the high purity of the composite particles, and the regular particle size and shape making this technique relatively simple (39).

1.8.8 Pulsed Laser Peposition (PLD)

This method is used in the production of many nanostructures such as nanorods, nanoparticles, as well as in the production of thin films, the nanostructure growth can be initiated via the solid-vapor mechanism through the production of nanoparticles in the gas phase at high pressures. The nanoparticles deposited on the substrate operate as nucleation sites, promoting the formation of nanostructures; the dimensions of the planted nanostructures are solely determined by the developing circumstances. (40).

The advantages of this method are its ability to generate a lot of energy, high-quality particles as well as low temperatures for the growth of substrates; it is also used to produce many nano-structures, such as nano-rod and nanowires. (41).

The working principle of PLD technology is based on the use of very short high-powered laser pulses of Nd YAG. The material is evaporated off the target, ionized, and deposited when a pulsed laser beam is concentrated inside of the vacuum chamber onto a solid target like ZnO. and the column is emitted to the target surface naturally. (42).

1.8.9 Chemical Vapor Deposition

Chemical vapor deposition (CVD) is a process that involves a chemical interaction between gaseous precursors and a substrate material's surface. The general process steps are depicted schematically as follows: 1) creation of the volatile carrier, 2) transportation of the volatile component by specific gases supplied into the system, and 3) chemical reaction on the substrate to generate a solid result. Thermal – CVD is the most prevalent type of CVD procedure. (43). The feedstock chosen should have a lower melting point than the substrate materials. In the semiconductor industry, this approach is commonly employed to manufacture high purity ratio, high achievement thin films and one-dimensional structures. Furthermore, when an unstimulated growth procedure is adopted, there is less chemical contamination. (44).

2. MATERIALS AND METHOD

2.1 Experimental

The production of ZnO NRs on different substrates (glass and p-Si) is described in this chapter. The dip-coating method is used to obtain ZnO seeds layers then the NRs are grown by hydrothermal process procedure.

2.1.1 Growth of ZnO NRs on the glass substrates

A homemade dip-coating system is built in the Materials Physics Laboratory, as represented in Figure (2.1), which is used to obtain the ZnO seed layer.

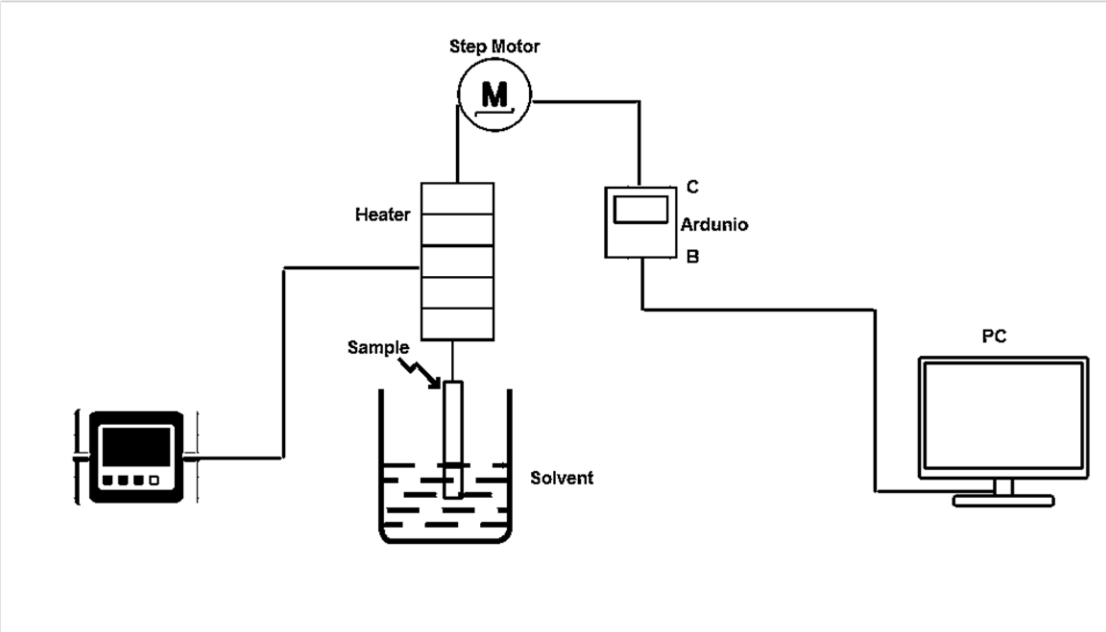

Figure.2.1. The Schematic of Dip Coating Device

2.1.1.1 Cleaning Samples

In the beginning, a sample of the glass was taken and cleaned; the cleaning process was repeated three times for each solution of acetone, ethanol, and propanol, where they are placed for 20 minutes under an ultra-sonication baths.

2.1.1.2 Preparation of ZnO Seed Layers

Dip-coating and annealing create a seed layer on a substrate, in this step, the seed layer solution was obtained by dissolving zinc acetate Zn $(CH_3CO_2)_2.2H_2O$ at a rate of 2.2 g and MEA in a concentration 0.6 ml in solution Me OH in concentration 40 ml. The Sol-gel was the process of deposition of zinc oxide for the growth of ZnO seed layers. After cleaning, the samples were dried with hot air, and then we started the coating process.

The seed layer was deposited on a layer of glass using a simple dipping coating process. The spin coats were done 10 times to achieve the desired thickness, and the sample was then annealed in an oven for 1 hour at 600°C. We compared the development rate and shape of ZnO NRs at temperatures of 540°C, 560°C, 580°C, and 600°C.

2.1.1.3 Growth of ZnO NRs by Hydrothermal Method

After the seed layer was deposited, the substrate was placed in an autoclave to develop ZnO NRs by melting zinc oxide in concentration 0.01m and hexamethylenetetramine (HMTA), ($C_6H_{12}N_4$) in concentration 0.1m were dissolved in a hydrothermal process and transferred to a Teflon-lined autoclave. Inside the autoclave, the substrate was preserved. For 3 hours, the autoclave was sealed and kept at a temperature of 90°C. The ZnO film was rinsed with DI water after growth to eliminate any leftover materials.

2.1.2 Growth of ZnO NRs on p-type Si substrates

We fabricated ZnO NRs by hydrothermal method on p-type Si (100) wafer and then make ohmic contact by using indium (In) wire.

2.1.2.1 Cleaning Samples

The silicon wafers were first cleaned by an ultrasonic device in a warm acetone bath for 20 minutes, then rinsed with deionized water. They were then placed in ethanol for 20 minutes in the ultrasonic bath, then rinsed with deionized water. Finally, they were put in propanol for 20 minutes and desiccated with nitrogen gas, to remove the primary oxide layer from the surface of the wafers, samples were etched wet for 10 seconds in hydrofluoric acid (HF: DI: 1:10) solution, washed with deionized water, and dried with nitrogen gas.

2.1.2.2 Preparation of ZnO Seed Layer

The ZnO seed solution was made using the Sol-gel technique. A fixative solution of zinc acetate dihydrate Zn $(CH_3COO)_2.2H_2O$ (2,19 g, 12 mmol) was dissolved in methanol 40 ml for 15 minutes and added to this monoethanolamine (MEA) 0.6 ml, 10 mmol solutions. After that, the solution was allowed to sit at room temperature for 8 hours to mix. The prepared solution was applied to the cleaned Si substrates. The films were then annealed at 600°C for 30 minutes.

2.1.2.3 Growth of ZnO NRs

After seed layer deposition, the substrate was transferred to an autoclave for ZnO NRs growth by using hydrothermal synthesis, where zinc dehydrate Zn $(CH_3COO)_2$ $2H_2O$, 0.1m was mixed with hexamethylenetetramine $C_6H_{12}N_4$, 0.1m in DI water (30 ml) at room temperature for 2 h. The substrate has been put within the autoclave, which was sealed for 3 hours at 90°C. After implantation, the ZnO film was washed with deionized water to remove any suspended material and then annealed in hot air at room temperature. Indium contacts were made on the surface of ZnO nanorods using a shadow mask picture 2.1 with round dots 1.5 mm diameter employing a thermo-physical vacuum coating technique on the surface of ZnO nanorods (Edwards-Auto 306) picture 2.2, with a pressure of 104 Pa, and high-purity indium was also vaporized on the other side of A schematic design of constructed In / ZnO/ p-type Si heterojunctions is shown in Figure (2.2).

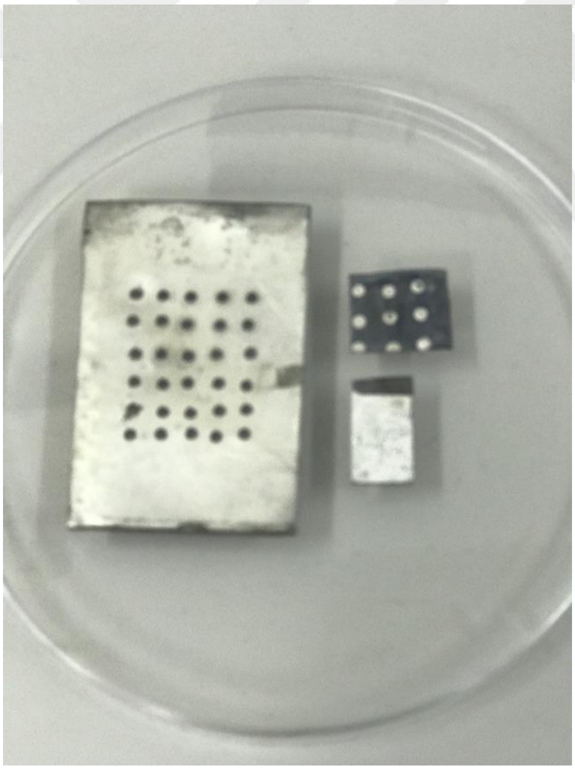

Picture 2.1 Shadow mask for making indium-ohmic contacts

Picture 2.2 Edwards-Auto 306 System

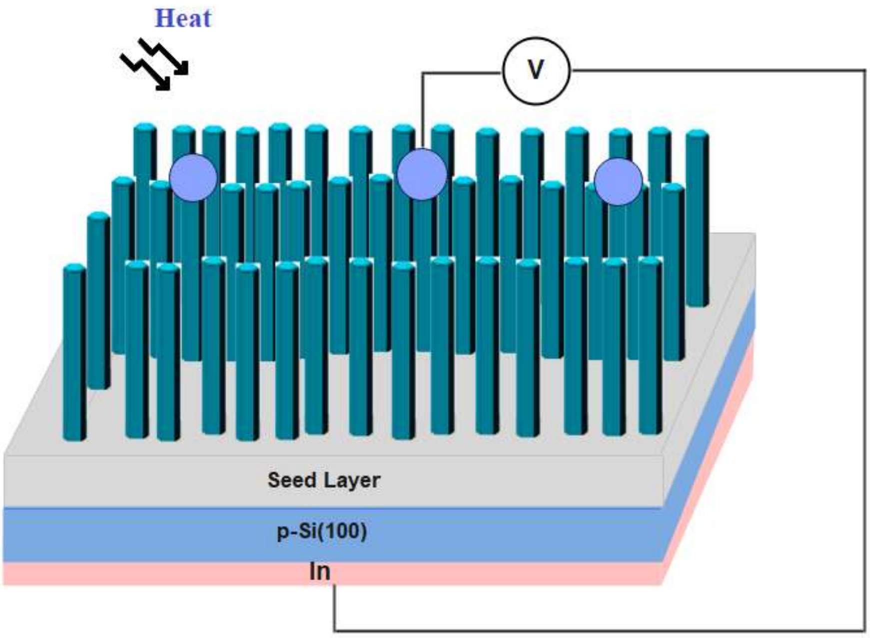

Figure 2.2. Schematics of seeding layer In / ZnO/ p-type Si substrate

3. RESULTS

This chapter starts with a brief description of the key principles behind the primary analytical techniques used for particle characterization (X-ray diffraction analysis, scanning electron microscopy (SEM), and UV analysis), as well as the analytical protocols used and a synopsis of specimen preparation for each of these procedures.

3.1 X-Ray Diffraction Results

X-rays are electromagnetic waves with a wavelength of approximately 1 angstrom (Å) (10^{-10} m). In the realm of material science, powder X-ray diffraction is a commonly used and important characterization technique. (45).

When accelerated electrons from a heated metal filament strike a metal source (in this case copper), distinctive X-rays are released, resulting in K_α and K_β emissions from the excited copper metal. Figure (3.1).

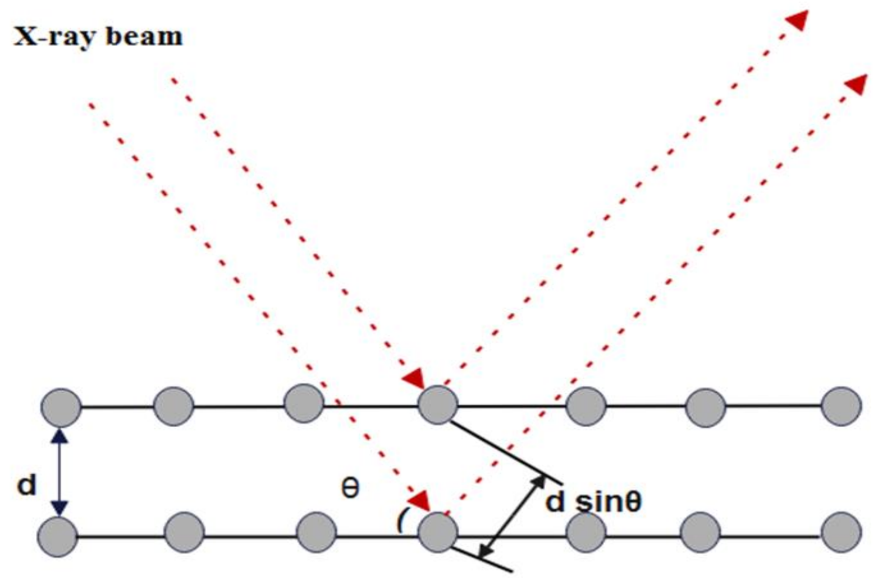

Figure. 3.1. Representation in a diagram of the principle of the x-ray diffraction.

Rigaku X-Ray Diffractometer device was used for this analysis. XRD patterns ZnO Figure 2.1 shows the XRD morphology of ZnO nanoparticles prepared on a glass substrate at 600°C. The XRD of all samples with 2θ values corresponds to reflectance planes at 31.89 (100), 34.41(002), 36.32(101), 47.56(102), 56.60(110), 62.69(103), confirms to JCPDS card number 36-1451, which are all compatible with zinc oxide with a wurtzite structure in our study. The high intensity of the (002) plane as compared to other planes clearly suggests the preferential growth of NRs along the c axis (46).

All diffraction peaks ZnO-NRs p-type Si (Fig 2.2) indicate wurtzite structure of hexagonal phase ZnO crystal (a = 3.249A˚, c = 5.206A˚, space group: P63mc (186)), in (Table 3.1) the comparison between the lattice parameters for ZnO/ glass and ZnO /Si.The diffraction peaks are placed at 002 and are in compliance with the Joint Committee on Powder Diffraction Standards of ZnO and the weak (100), (101), (102) and peaks are also observed match well with JCPDS data card No. 36-1451, silicon substrate peak (201) is also seen in the spectrum. For the sample characterized, the material's crystallinity is shown by the sharp and narrow diffraction peaks. (47). The mean size of ordered ZnO nanoparticles was calculated using the full width at half maximum (FWHM) and Debye-Scherer equations:

$$\mathbf{D} = \frac{\mathbf{k\lambda}}{\mathbf{B\ cos\theta}} \qquad 1.3$$

where k is Scherer's constant and its value is about 0.94, 0.154nm is the x-ray wavelength, B is the line broadening at half maximum intensity (FWHM) in radians, and θ is Bragg angle, according to the Debye-Scherer equation, the average size of the ZnO nanoparticles formed was (35.3) nm for ZnO with Glass substrate, and (30.16) nm for ZnO with Silicone substrate.

Picture 3.1. Rigaku Multiflex System Diffractometer

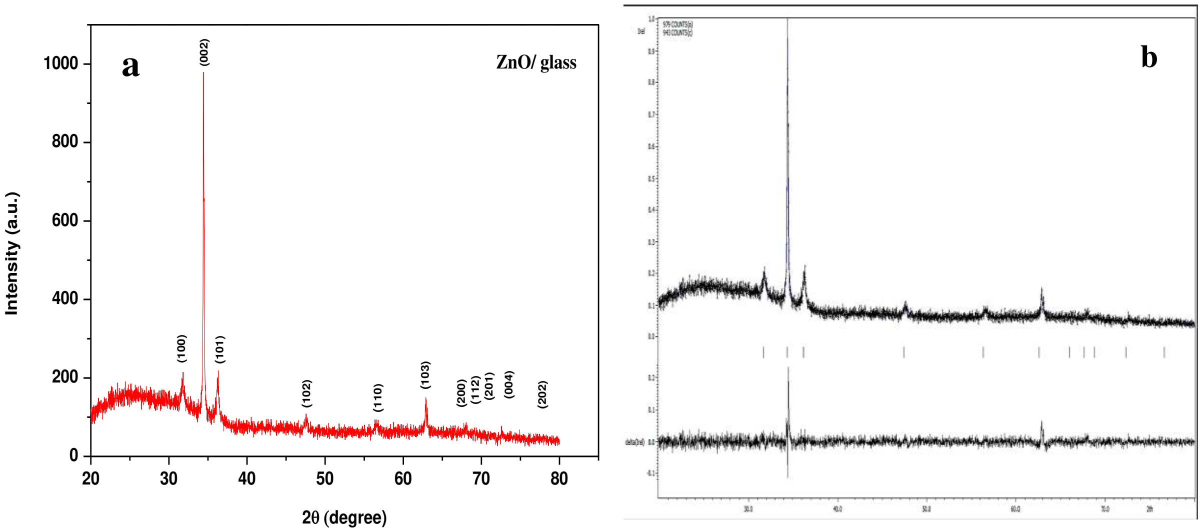

Figure.3.2. (a) XRD pattern for ZnO NRs on glass substrate. (b) Shown Rietveld refinements of ZnO, the experimental points are plotted in black line and theoretical data are shown as blue line. The difference between theoretical and experimental data is shown in the bottom line of each figure. The vertical lines represent the Bragg's allowed peaks

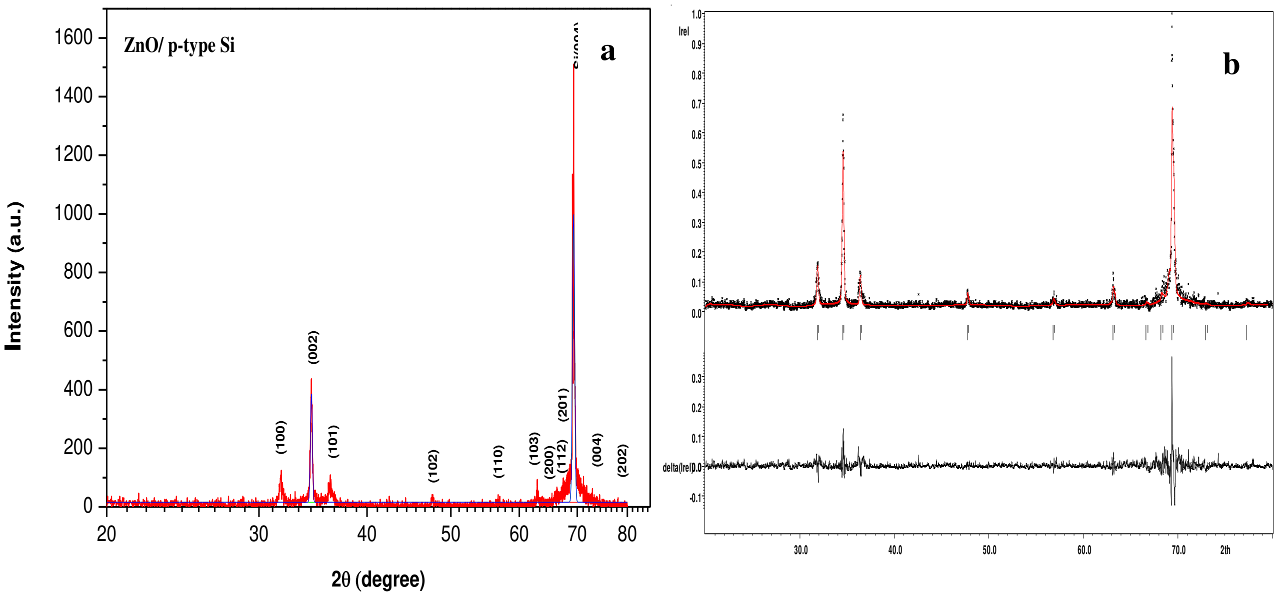

Figure 3.3. (a) XRD pattern for ZnO NRs on p tupe Si substrate. (b) Shown Rietveld refinements of ZnO, the experimental points are plotted in black line and theoretical data are shown as red line. The difference between theoretical and experimental data is shown in the bottom line of each figure. The vertical lines represent the Bragg's allowed peaks.

Table 3.1. Lattice parameters of ZnO NRs on different substrates and comparison lattice parameters of the JCPDS XRD database.

Sample	Lattice parameters		
	a (Å)	b (Å)	c (Å)
ZnO powder JCPDS	3.2498	3.2498	5.2066
ZnO/ glass	3.02782	3.02782	5.00417
ZnO/ p-type Si	3.23868	3.23868	5.18558

3.2 Scanning Electron Microscopy (SEM)

Scanning electron microscopy (SEM) allows researchers to investigate huge sample sizes in a short amount of time, making it ideal for analyzing particle morphology, size, and surface. The scanning electron microscope (SEM) can examine samples ranging in size from a few hundred micrometers to nanoparticles. In comparison to an optical microscope, the SEM offers greater resolution limitations and a far better depth of focus resolution (by a factor of 300). (49), in the scanning electron microscope, an electric gun produces a beam of high-energy electrons (up to 40 keV), A series of electromagnetic fields and lenses then focuses the light on a sample placed in a vacuum chamber. Scanning coils then scan the electron beam through the sample. (50).

When electrons hit the surface of the sample, reaction occurs with the atomic structure. Secondary electrons, background scattered electrons, and other components such as visible light and X-rays are among the radiation emitted during the process. Secondary electron (SE) and back scattered electron (BSE) emissions are the foundation of electron microscopy, and each type is studied separately. (51).

Fabrication of ZnO nanorods with morphological control. A hydrothermal technique was used to make varying sizes of 1-D ZnO nanorod structures by altering the precursor content and reaction temperature, in our study, we used a device type Quanta FEG 250 to take SEM images.

SEM pictures of samples developed at 560°C and 600°C on glass substrates revealed that the nanoparticles are mostly made up of ZnO nanorods, the results revealed that silicon was used as a substrate, and that the morphology of the silicon samples matched that of the glass samples.

Picture 3.2. Scanning Electrical Microscopy Device

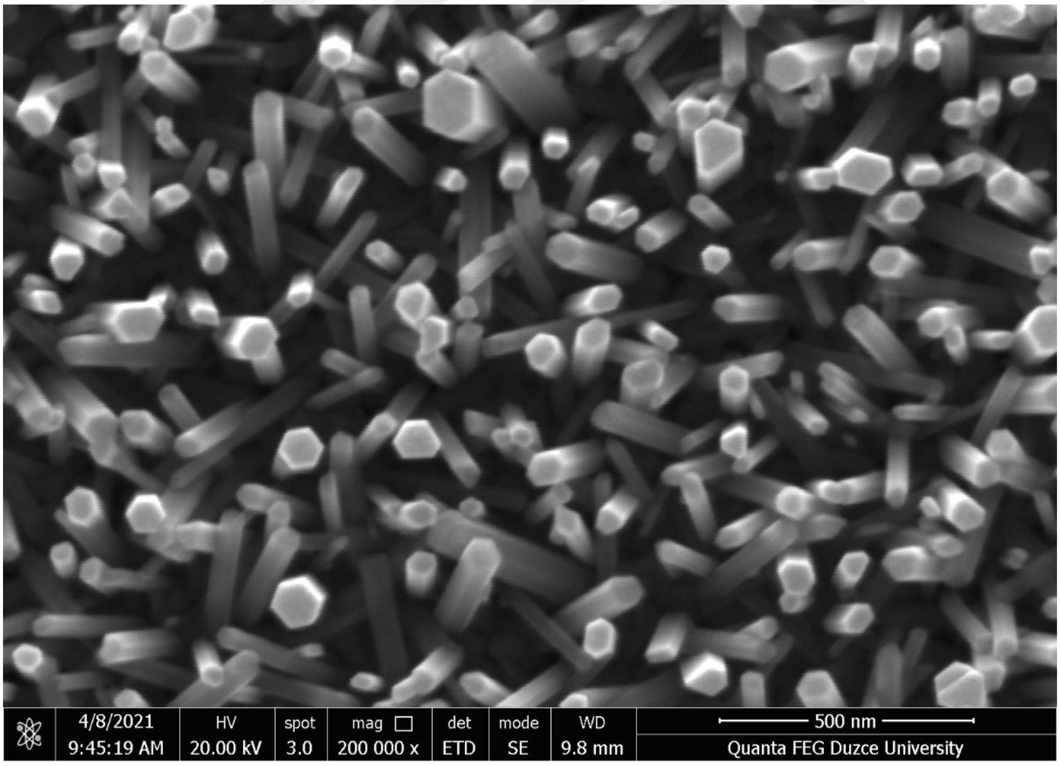

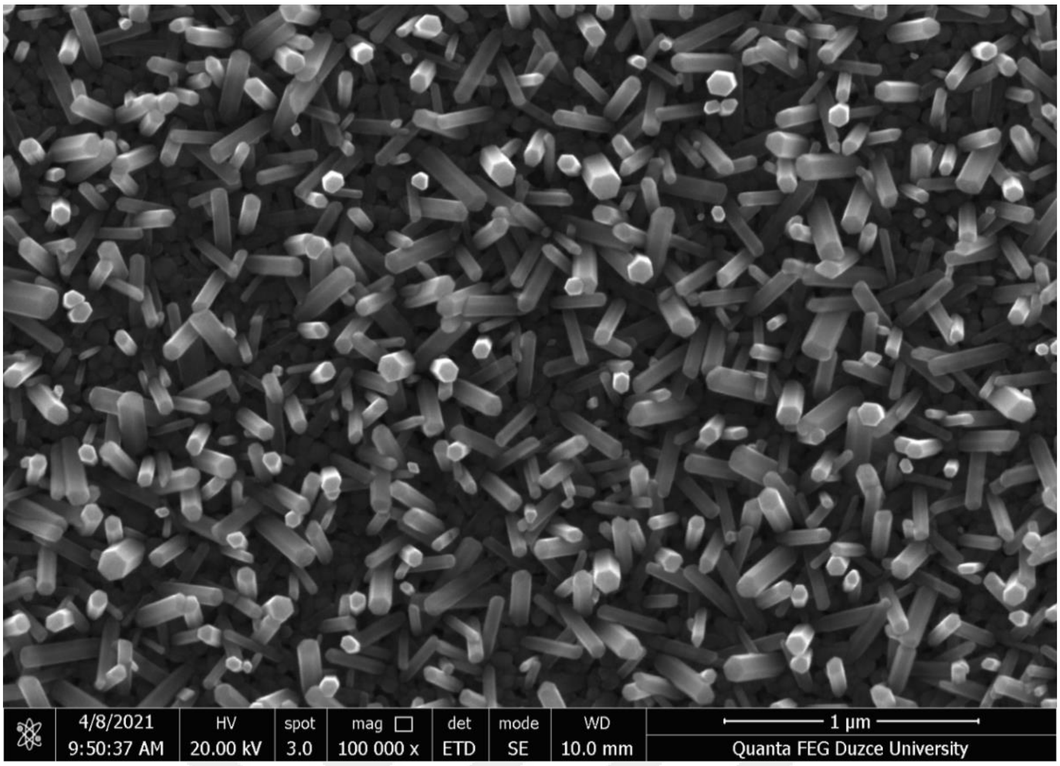

Figure 3.4. SEM top view images showing of ZnO nanoparticles grown on a glass substrate.

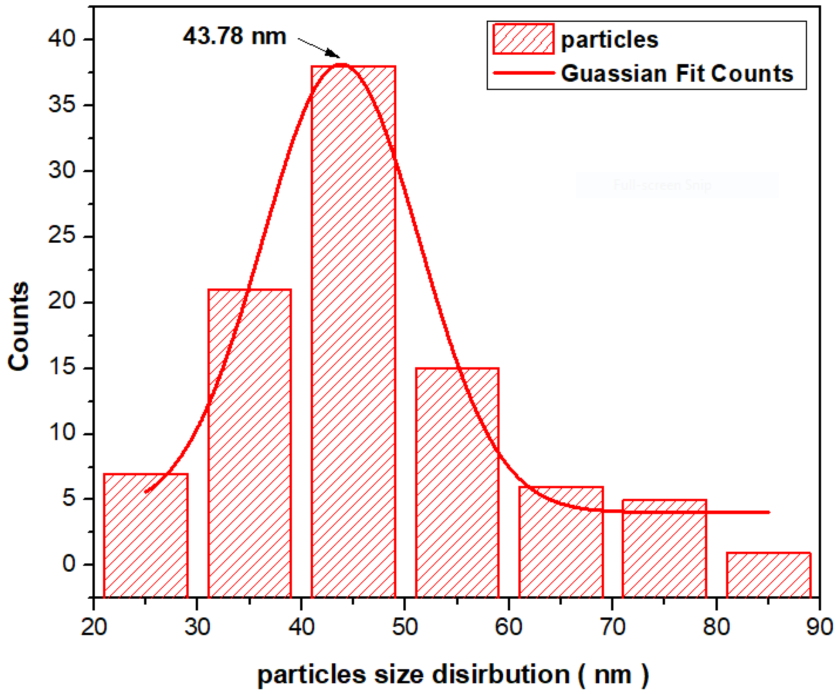

Figure 3.5. Grain size distribution of ZnO NRs grown on glass substrate diameter.

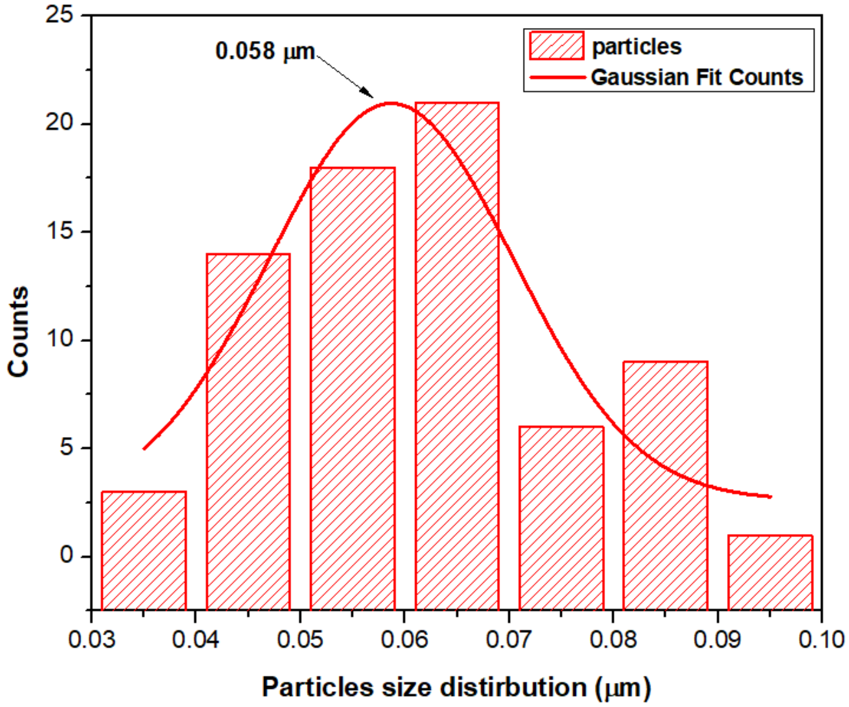

Figure 3.6. Grain size distribution of ZnO NRs grown on glass substrate length.

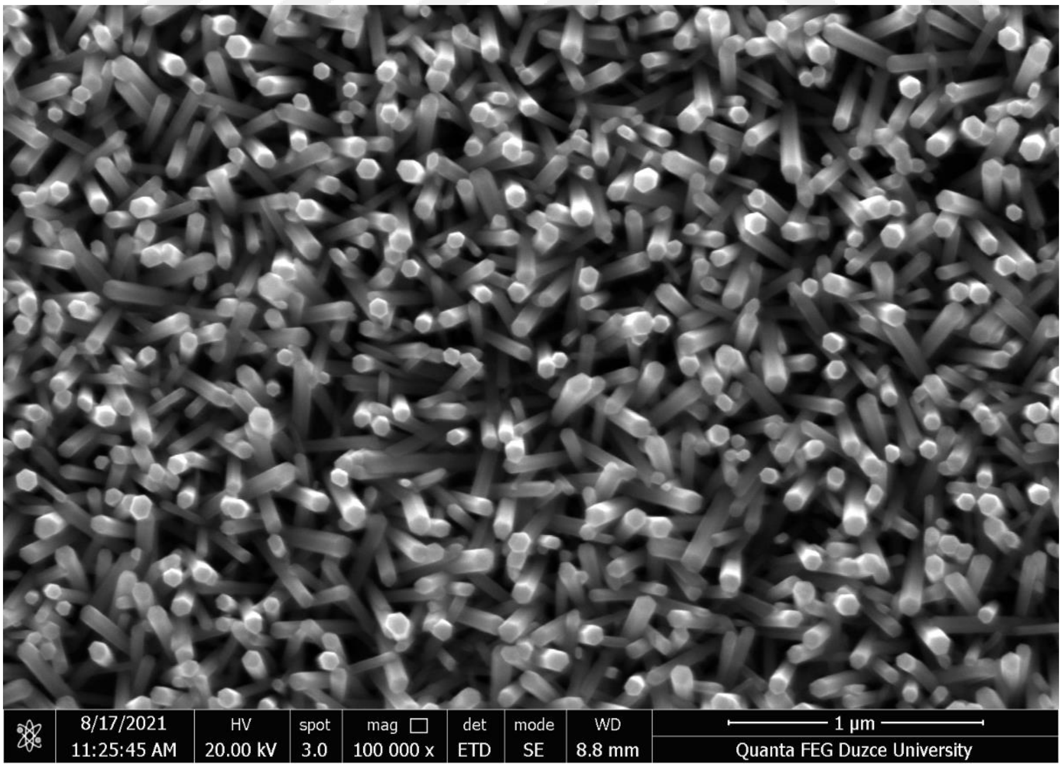

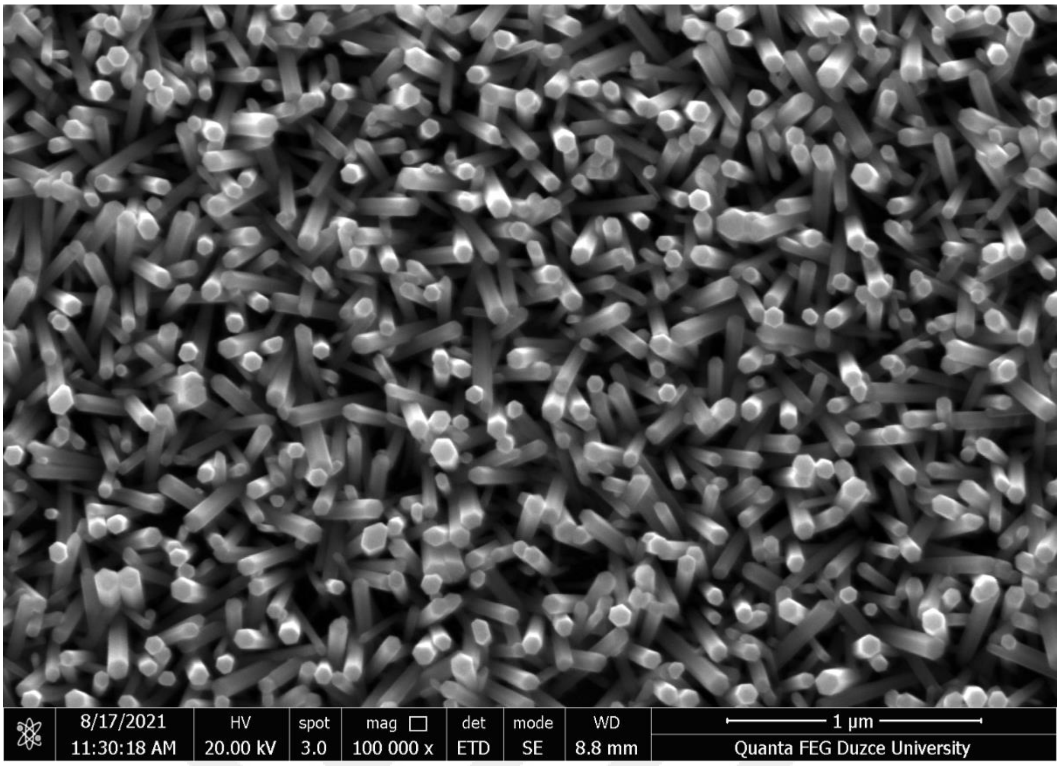

Figure 3.7. SEM top view images of ZnO nanoparticles grown on a Silicone substrate.

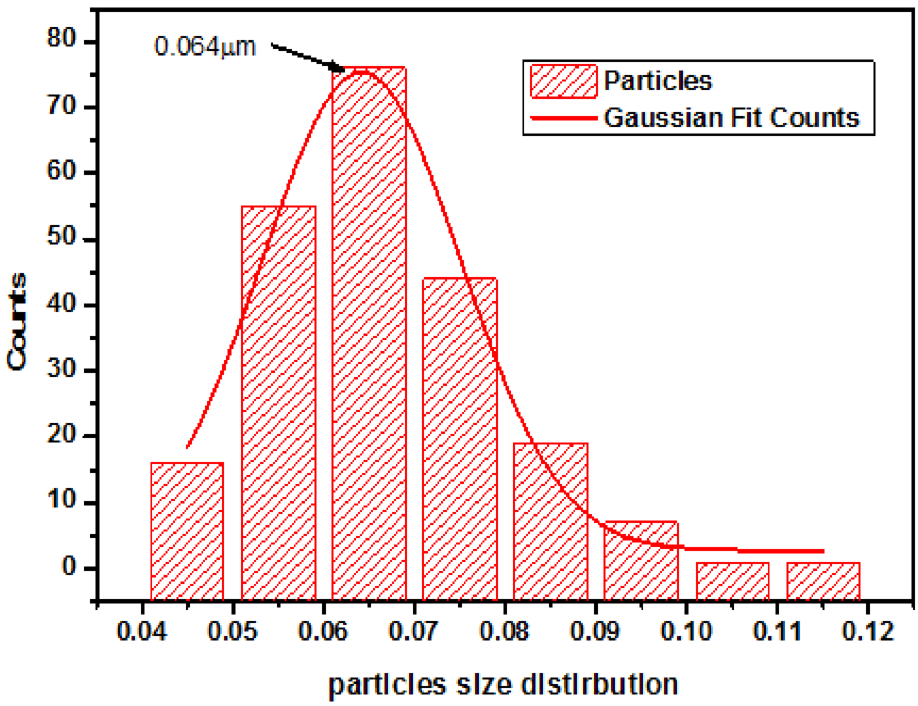

Figure 3.8. Grain size distribution for ZnO NRs on p- type Si substrate diameter.

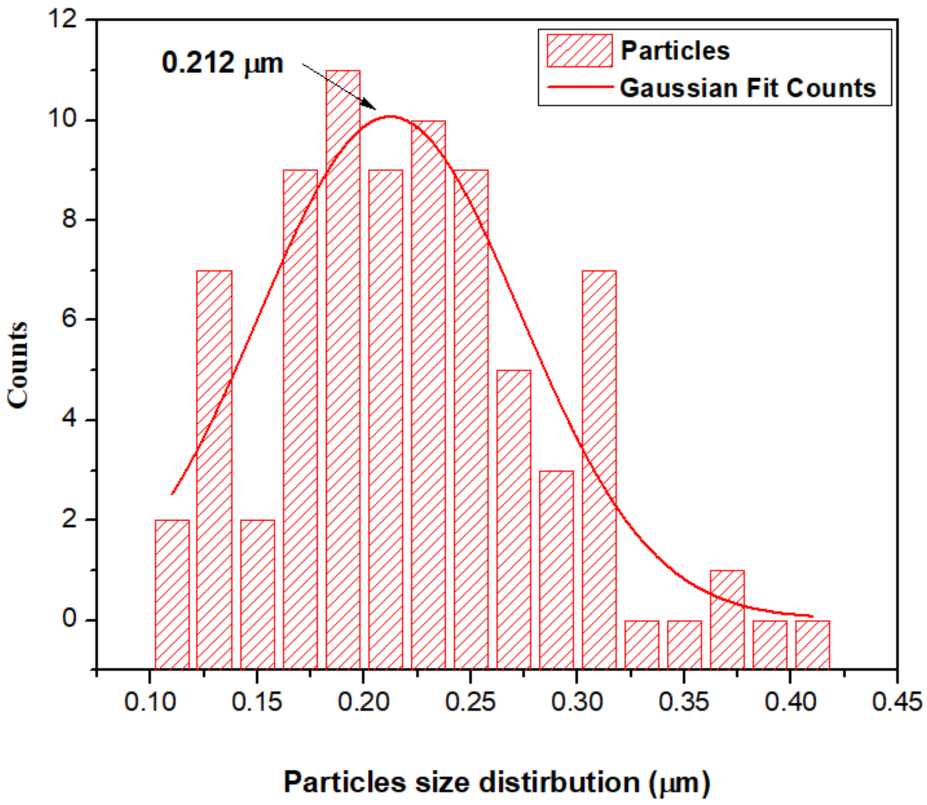

Figure 3.9. Grain size distribution for ZnO NRs on p-type Si substrate length.

SEM images of ZnO NRs grown on glass and p-type Si substrates presented in Figures (3.4, 3.7). The photos show creation nanorods that are oriented perpendicularly and have varying aspect ratios. Nanorods generated on glass substrates, for example (Figures. 3.5 and 3.6) it has an average diameter 43.78 nm and 58 nm in length because because the ZnO NRs are dependence of mainly on the grain size of seeds layers. (52), while those that grow on Si substrates (Figures. 3.8 and 3.9) are found with average length 212 nm and 64 nm in diameter, this suggests that the kind of substrate affects the side ratio of single-crystal ZnO nanorods in the (002) direction. This could be due to a different misfit between the seed and each ZnO substrate. (53).

3.3 Optical Properties

3.3.1 FT-IR Spectrum Analysis of ZnO

To describing the surfaces of nanoparticles, Fourier transform infrared is a very useful technique, it is possible to evaluate the surface chemical composition of nanoparticles under certain conditions, and it is also possible to determine the reactive surface sites responsible for the interaction of surfaces, as for the FTIR spectrum, it ranges between 4000 and 400 cm^{-1} values. A Shimadzu 2600 UV spectrophotometer and Fourier transform infrared (FTIR) probes were used to determine it.

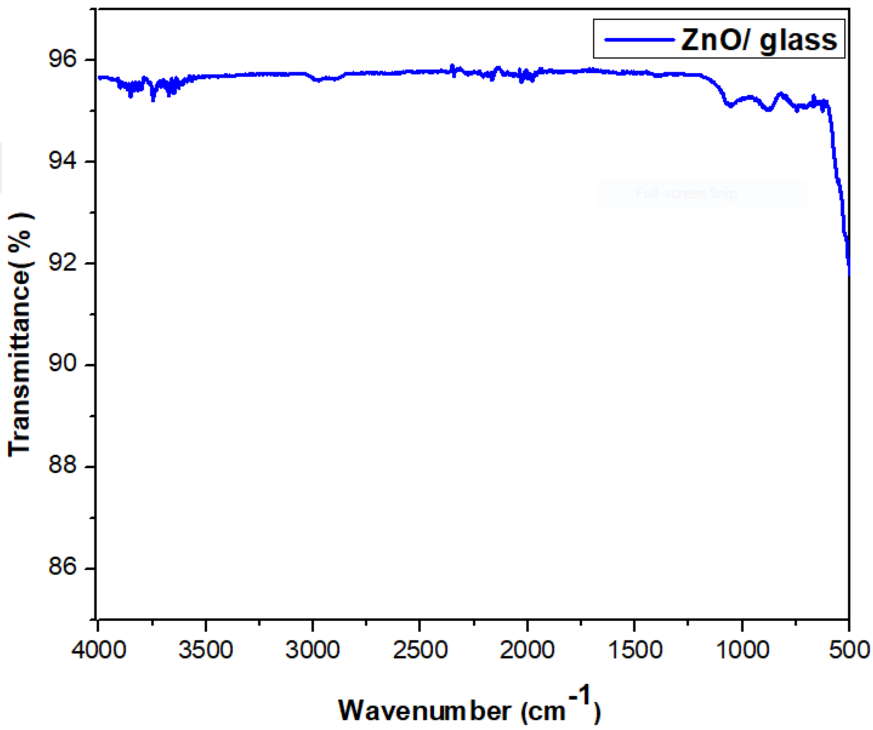

Figure 3.10. FT-IR spectra of the prepared ZnO NRs with glass substrate.

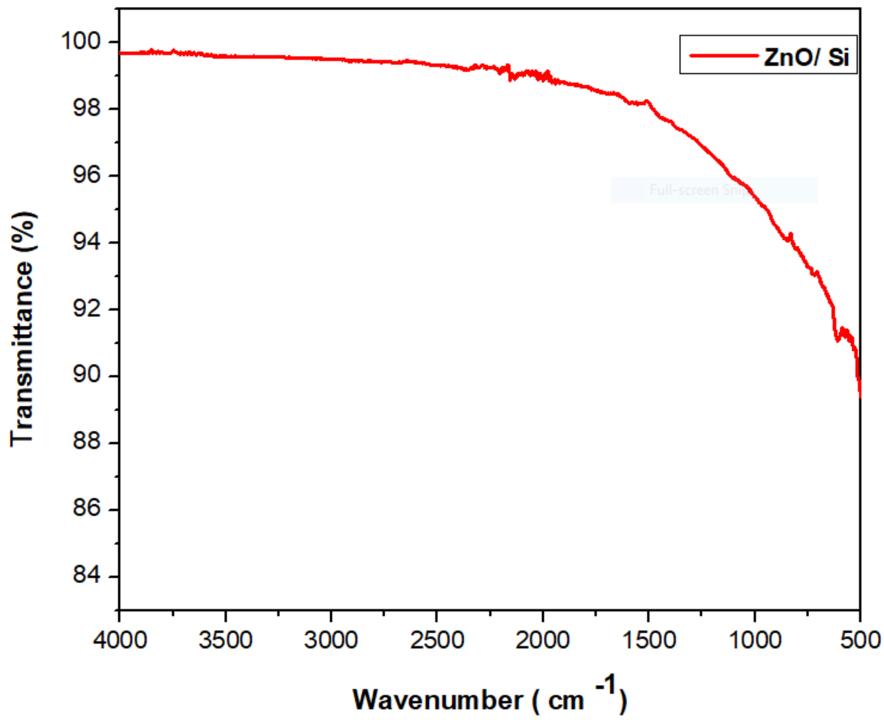

Figure 3.11. FT-IR spectra of the prepared ZnO NRs with the p- type Si.

Shown in the Figure 3.10 is the FTIR pattern of zinc oxide on a glass substrate, generated using the hydrothermal process between 2846 and -1184 $cm-^{1}$, while peaks appeared in the sample that used Silicon as a substrate ranging between 2171cm^{-1} and 4000 cm^{-1} in Figure 3.11 and ester bonding is shown by the adsorption band at 1060 cm^{-1} for glass, as for silicon, it was observed that the visible absorption occurred 1980 cm^{-1}. (54).

3.4 Electrical Properties

3.4.1 Capacitance and Conductivity

ZnO variants offer excellent nonlinear conductivity and have been utilized in surge protection devices for a long time. The capacitive impact of conduction current under time-varying fields is attributed to varied conductors and the so-called nonlinear permittivity in certain research. (55).

The In/ZnO/p-type Si heterostructure's capacitance–voltage and conductivity–voltage experiments were carried out at various frequencies to evaluate the heterostructure's essential electrical and dielectric properties, the measured capacitance is dependent on the applied voltage in addition to the frequency that is included, as seen in Figure 3.12, the accretion logic, attrition area, and reflection area are the three systems that make up C – V curves, there is a certain degree of axis state offset due to the presence of surface stats, because there are impacts such as percentage of impurities present and high resistance in addition to the amount of doping, the voltage dependent amplitude decreased when the applied frequencies were increased, the interface states follow the AC signal at lower frequencies, resulting in an increase in capacitance, the cause for the frequency dispersion that happened is related to the state of the interface, density distribution of the ZnO/p-type Si interface and its relaxation lifetime as a result of the bias in the voltage, the scattering tendency was detected in both the negative and positive voltage areas of the G-V curve as shown in Fig 3.13, and there was an increase in voltage with increasing frequency and a noticeable drop in the superposition zone.

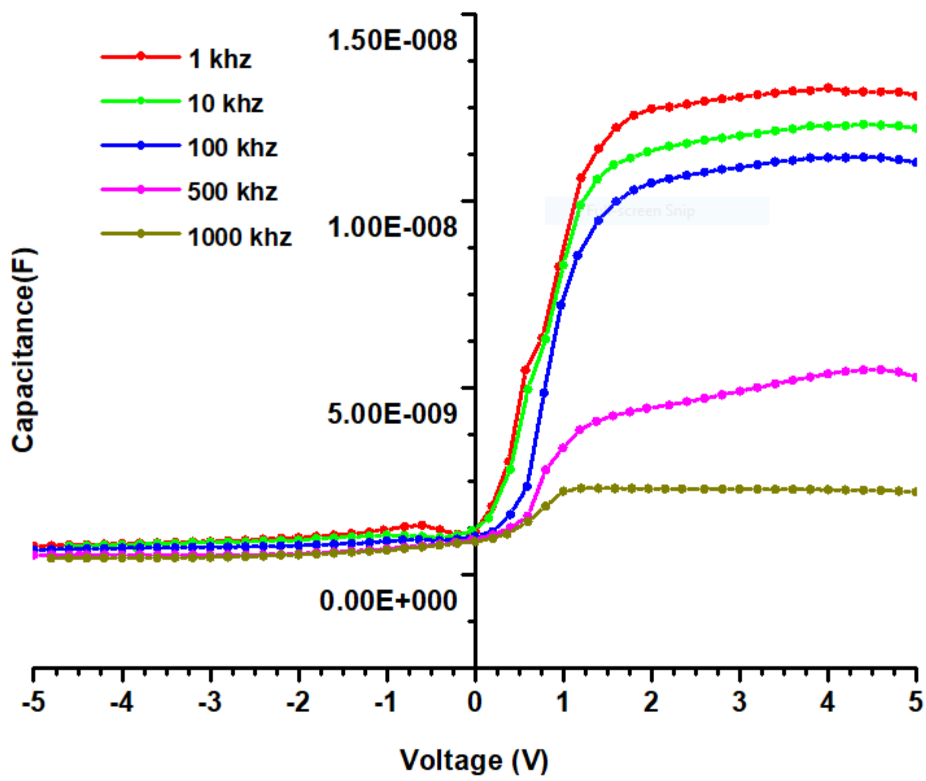

Figure 3.12. C–V relation of the ZnO /p-Si dependence of measurement frequency

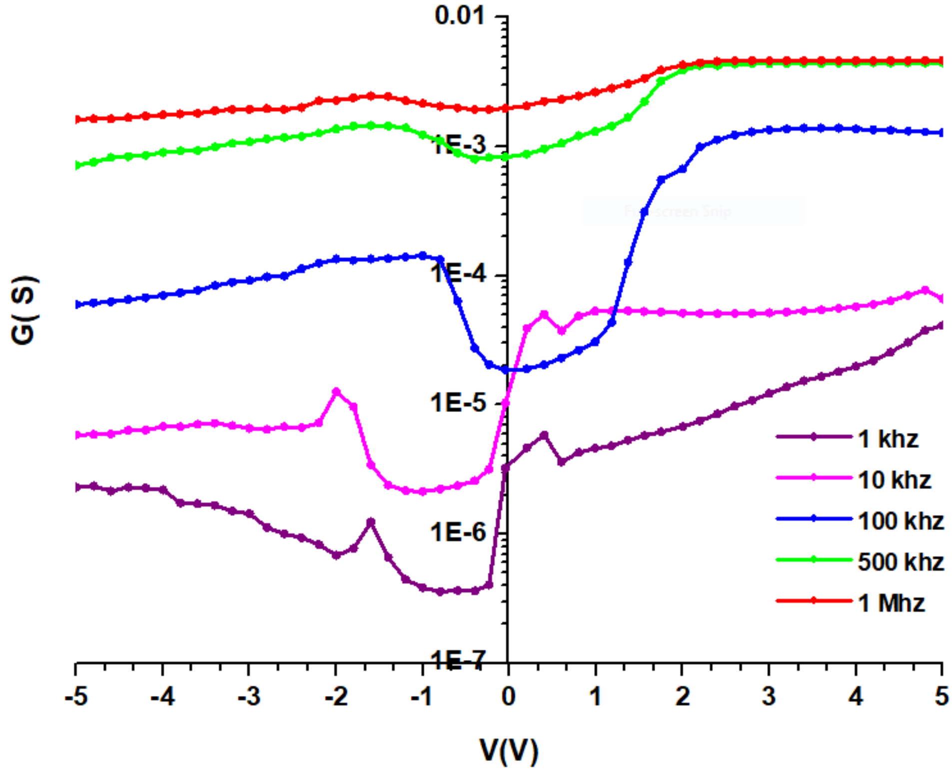

Figure 3.13. Measurement of conductivity (G) as a function of voltage(V) under different frequencies.

3.4.2 Dielectric Permittivity

Computer-controlled software was used to measure capacitance and dielectric loss tangent (tanδ) at frequencies ranging from 1 kHz to 1 MHz over a wide voltage range. As electrodes, measurements were made on circular plate-shaped samples with indium plating on two sides, the real (ε') and imaginary (ε") parts of the complex dielectric constant were calculated using raw data and the relevant sample dimensions as follows:

$$\varepsilon' = \frac{Ct}{\varepsilon_0 A} \quad \text{and} \quad \varepsilon'' = \varepsilon' \tan\delta \qquad 2.3$$

where C is the capacitance (F), t is the sample thickness (m), A is the cross-sectional area (m^2), and ε_o is the free space permittivity (ε_o= 8.854 10^{-12} F/m). (56). Figure 3.14, 3.15 the ZnO/p-Si heterostructure's the real (ε′) and imaginary parts (ε″) of the complex permittivity as a function of Frequency (10 khz to 1 MHz) under different Voltages ranging from (5 V to +5 V).

When applying voltages less than V0, the real permittivity is almost constant, then it grows with higher voltages, but we notice a significant decrease in the value of ε' in the high frequency region starting at 100 kHz, as shown in Figure (3.14). The value of ε″ is almost constant at low frequencies and then increases with increasing voltage at high frequencies, the effect of the nanocomposites' high DC conductivity is responsible for the high levels, according to studies.. High dielectric constants were obtained in several experiments utilizing nanostructured ZnO.

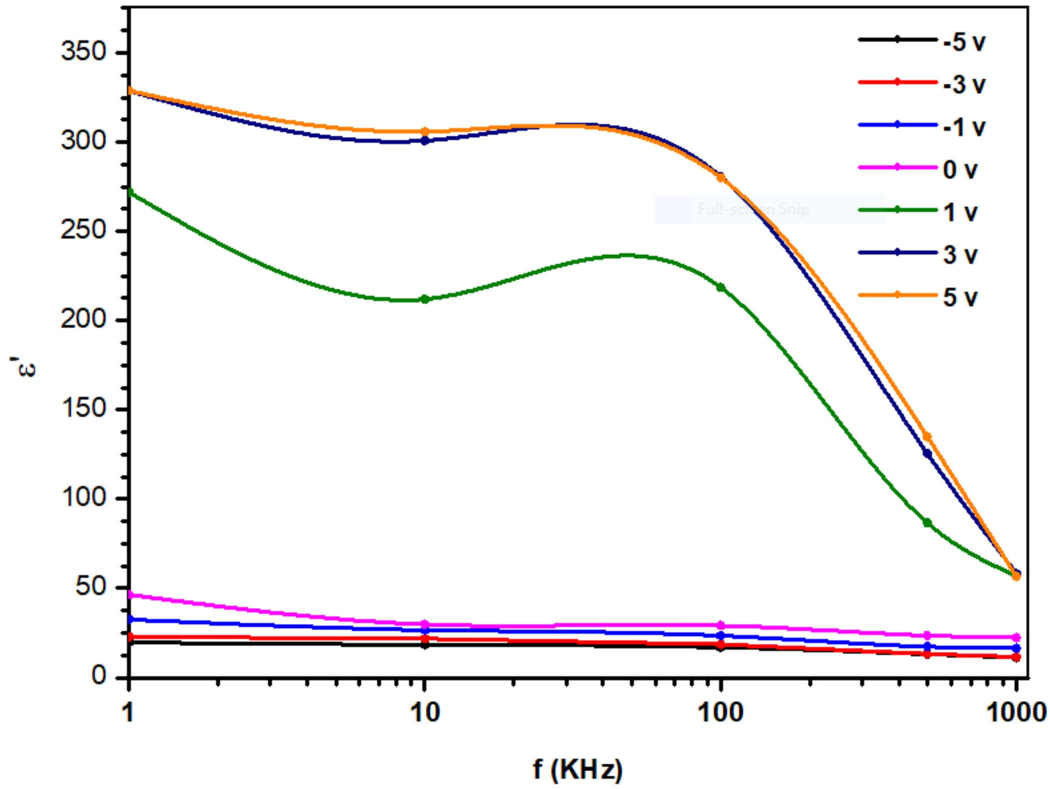

Figure 3.14. At various Voltages, Frequency dependency on the real part dielectric permittivity *ε*' of In/ ZnO NRs /p- type Si.

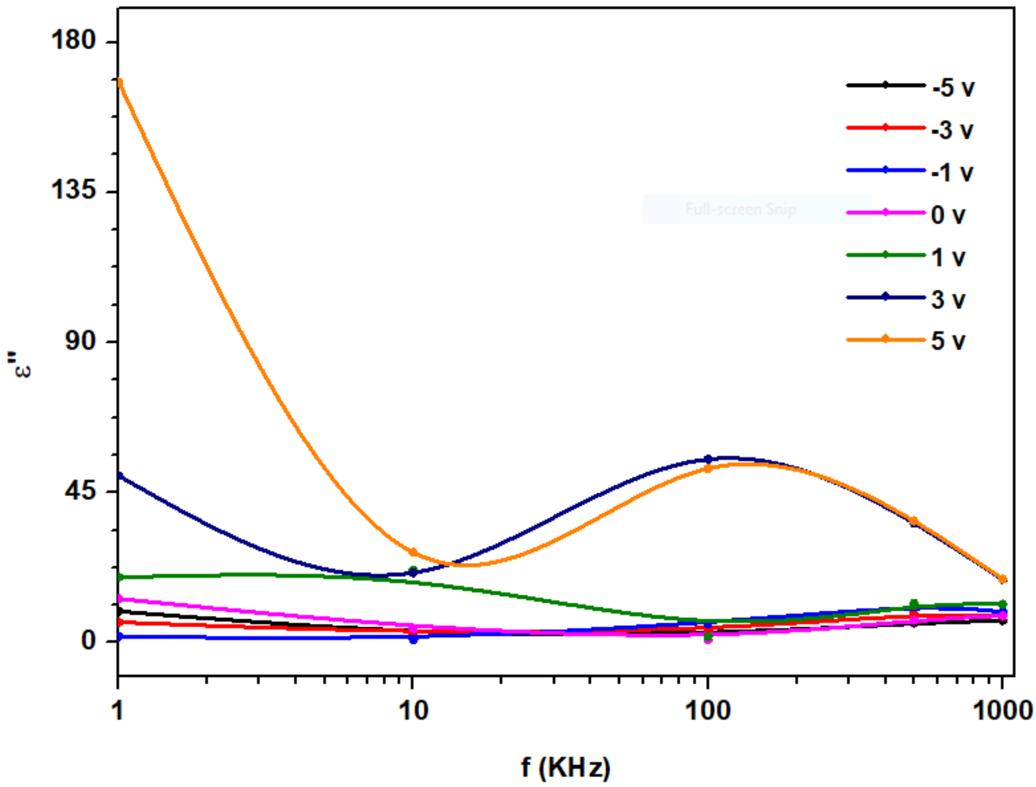

Figure 3.15. Frequency dependence on the imagine part dielectric permittivity ε'' at different voltage of In/ ZnO NRs /p-type Si.

Figure 3.16 shown the fluctuation in the value of the dielectric loss tangent as a function of frequency for the ZnO /p-Si sample when applied under different frequencies, a significant decrease in the value of ($\tan\delta$) was observed. ion hopping and electronic polarization, as well as space charge polarization, cause this behavior that is comparable to that of the dielectric constant.

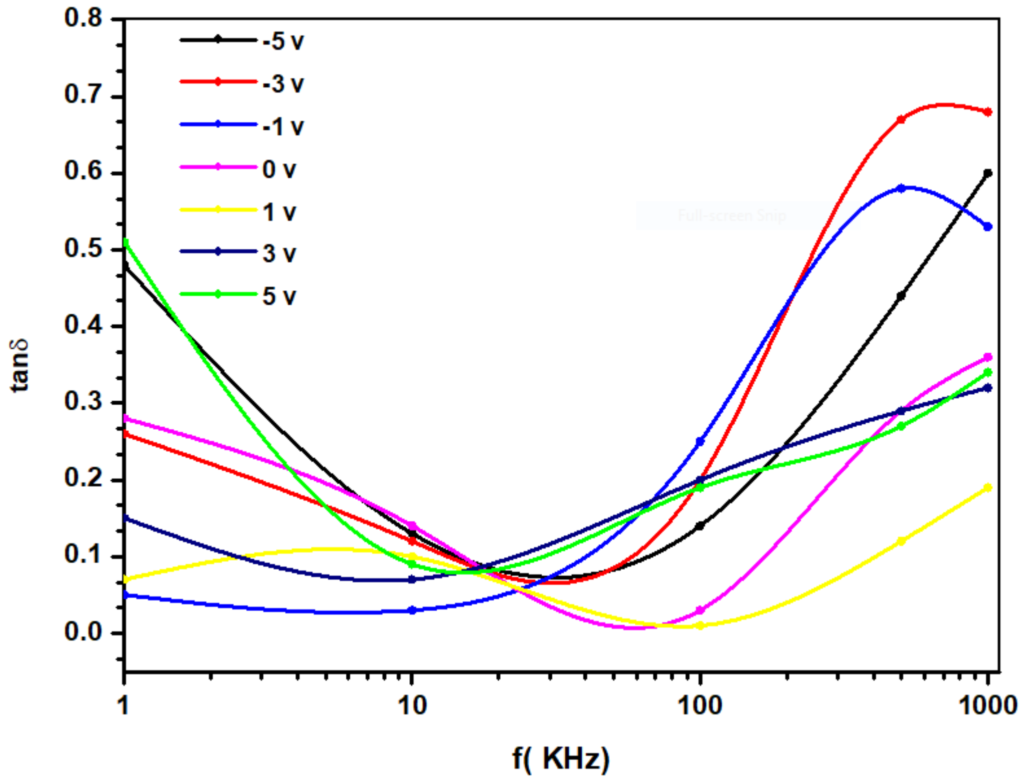

Figure 3.16. Graph between the tangent of loss tanδ and frequency under different voltages for the In/ZnO/p-type Si heterogeneous structure

3.4.3 Electric Modulus

Usually, electrophoretic spectroscopy is extremely beneficial for understanding conduction pathways and identifying microscopic processes that cause dielectric relaxation and polarization. As a result, many scientists prefer to use the electrical modulus formula to describe dielectric behavior with frequency. (57).

The mechanism of relaxation of the electric field in a sample when the electric displacement remains constant is the physical significance of the electric modulus. (58).

The complex electrical modulus (M *) is used for this. which is known as the reciprocal of complex permittivity (ε*):

$$M^* = M' + iM'' \quad 3.3$$

$$M^* = \frac{1}{\varepsilon^*} = \frac{\varepsilon'}{\varepsilon'^2+\varepsilon''^2} + i\frac{\varepsilon''}{\varepsilon'^2+\varepsilon''^2} \quad 4.3$$

Where M' and M'' are the real and imaginary components of the electric modulus. (59).

The real (M') and imaginary (M") components complex electric modulus of the In/ZnO/p-Si heterostructure's are shown in Fig. 3.17 and Fig. 3.18, the modulus versus frequency curves for positive voltages lack a clear frequency and voltage dependent distribution, On the contrary, there was a frequency and voltage dispersion in the negative voltage region. According to the applied voltages, the M' ratios rise with increasing frequency, which means that the polarization decreases and the dipoles relax. (60).

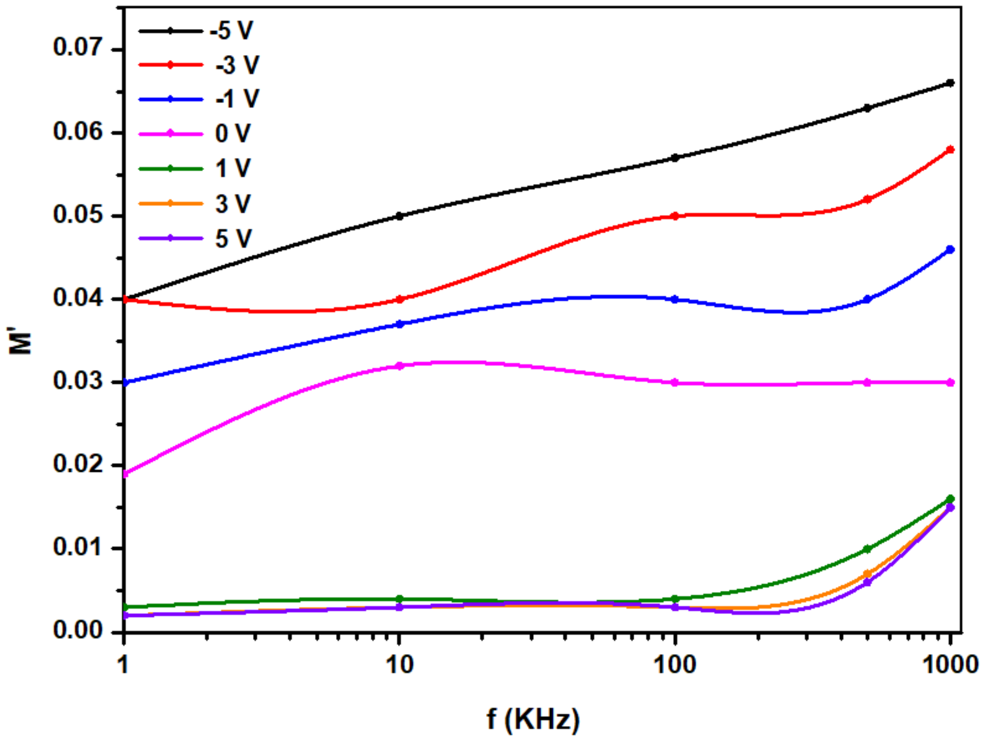

Figure 3.17. The real part of modulus (M') for ZnO /p-type Si nanoparticles as a function of frequency with deferent voltages.

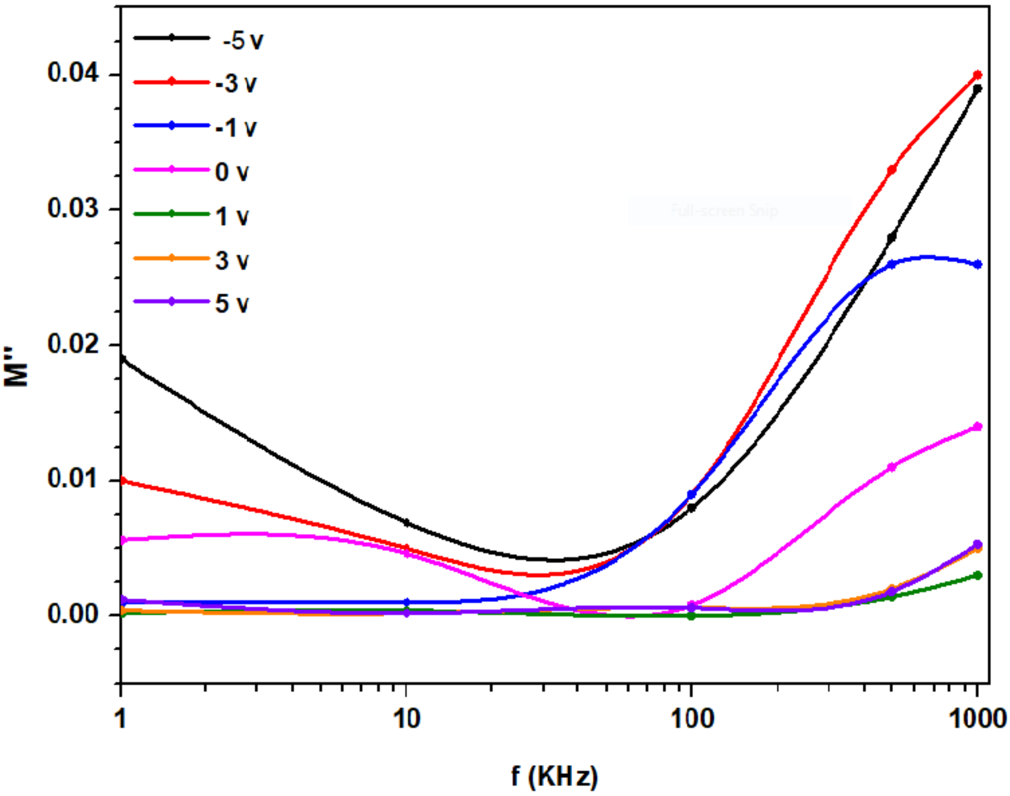

Figure 3.18. The imaginary part of modulus (M'') for ZnO /p-type Si nanoparticles as a function frequency with deferent voltages.

4. CONCLUSIONS AND RECOMMENDATIONS

ZnO NRs are grown on glass and p-Si substrates by hydrothermal method and the structural and morphological properties of the grown ZnO NRs were depicted by using XRD and SEM techniques. The LeBail refined XRD patterns of the fabricated films show that all films crystallized in the wurtzite (hexagonal) structure (JCPDS card no. 36-1451) with $P6_3mc$ space groups and the preferred growth direction of ZnO NRs is in the c-axis orientation. No other impurity peaks were detected indicating a pure ZnO layer. The average hexagonal diameter of the films are obtained about 43 and 64 nm for glass and Si substrates, respectively. These results confirm the nanorod morphology of ZnO film.

For electrical transport properties, the capacitance and conductivity measurements are performed for the fabricated In/ZnO/p-Si heterojunction. The capacitance measurements were shown as a function of voltage under frequency values between 1 and 1000 kHz and the capacitance results showed a response to high frequencies in the positive voltage region, while the conductivity results showed a response in both negative and positive regions, due to the effect of polarization mechanisms, results of the relative permittivity ε' , $\varepsilon''$and loss tangent ($\tan\delta$) were in the positive voltage range, there is a significant frequency dependence of the values ε' and ε'', in the region of negative voltage, they tend to approach a constant value that is practically frequency-independent, $\tan\delta$ is usually high at the low and high frequencies since it is usually low in the middle frequency range from 10kHz to 100kHz, the frequency dependency of these space charge polarization was suggested as the cause of the shifting behavior in the ε' , $\varepsilon''$and $\tan\delta$ with frequency.

Electric modulus readings while there is a frequency and voltage dispersion for negative voltages, the M′-f curves for positive voltages do not clearly display a frequency and voltage-dependent distribution.

5. REFERENCES

"Vancouver citation system was used in this thesis."

1. Kim I, Viswanathan K, Kasi G, Thanakkasaranee S, Sadeghi K, Seo J. ZnO Nanostructures in Active Antibacterial Food Packaging: Preparation Methods, Antimicrobial Mechanisms, Safety Issues, Future Prospects, and Challenges. Food Reviews International. 2020 Mar 9;1–29.
2. Willander M, ul Hasan K, Nur O, Zainelabdin A, Zaman S, Amin G. Recent progress on growth and device development of ZnO and CuO nanostructures and graphenenanosheets. J Mater Chem. 2012;22(6):2337–50.
3. Kołodziejczak-Radzimska A, Jesionowski T. Zinc Oxide—From Synthesis to Application: A Review. Materials. 2014 Apr 9;7(4):2833–81.
4. Farhat OF, Halim MM, Abdullah MJ, Ali MKM, Allam NK. Morphological and structural characterization of single-crystal ZnO nanorod arrays on flexible and non-flexible substrates. Beilstein Journal of Nanotechnology. 2015 Mar 12;6:720–5.
5. Wang ZL. Zinc oxide nanostructures: growth, properties and applications. Journal of Physics: Condensed Matter. 2004 Jun 30;16(25):R829–58.
6. Willander M, ul Hasan K, Nur O, Zainelabdin A, Zaman S, Amin G. Recent progress on growth and device development of ZnO and CuO nanostructures and graphenenanosheets. J Mater Chem. 2012;22(6):2337–50.
7. 'Altıntaş Yıldırım Ö. SYNTHESIS OF ZINC OXIDE NANOPARTICLES BY AQUEOUS METHODS AND EFFECT OF METAL INCORPORATION ON THE STRUCTURAL/FUNCTIONAL PROPERTIES OF NANOPARTICLES. [Turkey]: MIDDLE EAST TECHNICAL UNIVERSITY; 2014.
8. Klingshirn C. ZnO: From basics towards applications. physica status solidi (b). 2007 Sep;244(9):3027–73.
9. 'Behera O. Synthesis and Characterization of ZnO nanoparticles of various sizes and Applications in Biological systems. [Orissa, India]: National Institute of Technology Rourkela; 2011.
10. 'MOHAMMED ALI N. Study of Structural and Optical Properties of (ZnO:Sn)Thin Films Prepared By Chemical Spray Pyrolysis Method. [Diyala, Iraq]: Diyala University in partial fulfillment of the requirements; 2010.
11. Coleman VA, Jagadish C. Basic Properties and Applications of ZnO. In: Zinc Oxide Bulk, Thin Films and Nanostructures. Elsevier; 2006. p. 1–20.
12. Farahbod F, Farahmand S. Empirical Investigation of Heating and Kinematic Performance of ZnO Nano Fluid in a Heat Pipe. Journal of Nanofluids. 2017 Feb 1;6(1):128–35.
13. New Jersey Department of Health, Cresswell A. Right to know: Hazardous substance fact sheet [Internet]. New Jersey Department of Health. 2008. Available from: www.cdc.gov/niosh/topics/ctrlbanding/.
14. Wu F, Harper BJ, Harper SL. Comparative dissolution, uptake, and toxicity of zinc oxide particles in individual aquatic species and mixed populations. Environmental Toxicology and Chemistry. 2019 Mar 18;38(3):591–602.
15. Hellen N, Park H, Kim KN. Characterization of ZnO/TiO2 Nanocomposites Prepared via the Sol-Gel Method. Journal of the Korean Ceramic Society. 2018 Mar 31;55(2):140–4.
16. Reed RB, Ladner DA, Higgins CP, Westerhoff P, Ranville JF. Solubility of nano-zinc oxide in environmentally and biologically important matrices. Environmental Toxicology and Chemistry. 2012 Jan;31(1):93–9.
17. You HC. Transistor characteristics of zinc oxide active layers at various zinc acetate dihydrate solution concentrations of zinc oxide thin-film. Journal of Applied Research and Technology. 2015;13(2).
18. 'Behera JK. SYNTHESIS AND CHARACTERIZATION OF ZnO NANO-PARTICLES. [ORISSA, INDIA]: NATIONAL INSTITUTE OF TECHNOLOGY, ROURKELA; 2009.

19. Kato H, Sano M, Miyamoto K, Yao T. Growth and characterization of Ga-doped ZnO layers on a-plane sapphire substrates grown by molecular beam epitaxy. Journal of Crystal Growth. 2002 Apr;237–239:538–43.
20. Özgür Ü, Alivov YaI, Liu C, Teke A, Reshchikov MA, Doğan S, et al. A comprehensive review of ZnO materials and devices. Journal of Applied Physics. 2005 Aug 15;98(4):041301.
21. ’ Paul Harvey J. Optoelectronic properties of highly mismatched semiconductor materials. [Uk]: University of Warwick; 2009.
22. Dulub O, Boatner LA, Diebold U. STM study of the geometric and electronic structure of ZnO()-Zn, ()-O, (), and () surfaces. Surface Science. 2002 Nov;519(3):201–17.
23. Kisi EH, Elcombe MM. u parameters for the wurtzite structure of ZnS and ZnO using powder neutron diffraction. Acta Crystallographica Section C Crystal Structure Communications. 1989 Dec 15;45(12):1867–70.
24. Kim I, Viswanathan K, Kasi G, Thanakkasaranee S, Sadeghi K, Seo J. ZnO Nanostructures in Active Antibacterial Food Packaging: Preparation Methods, Antimicrobial Mechanisms, Safety Issues, Future Prospects, and Challenges. Food Reviews International. 2020 Mar 9;1–29.
25. Polsongkram D, Chamninok P, Pukird S, Chow L, Lupan O, Chai G, et al. Effect of synthesis conditions on the growth of ZnO nanorods via hydrothermal method. Physica B: Condensed Matter. 2008 Oct;403(19–20):3713–7.
26. Pyskio L, Pawlowski P, Nieinski K, Slusarski L, Wlodarska M, Bak C. Study on reduction of zinc oxide level in rubber compounds - part II mechanism of activation of sulphur vulcanisation by means of the interphase transfer catalyst 18-crown-6-ether. KGK Kautschuk Gummi Kunststoffe. 2008;61(9).
27. Moezzi A, McDonagh AM, Cortie MB. Zinc oxide particles: Synthesis, properties and applications. Vols. 185–186, Chemical Engineering Journal. 2012.
28. Ohyama M, Kouzuka H, Yoko T. Sol-gel preparation of ZnO films with extremely preferred orientation along (002) plane from zinc acetate solution. Thin Solid Films. 1997 Aug;306(1):78–85.
29. Wang X. Preparation, Synthesis and Application of Sol-Gel Method. Faculte Des Sciences Montpellier. 2020.
30. Liu B, Zeng HC. Hydrothermal Synthesis of ZnO Nanorods in the Diameter Regime of 50 nm. J Am Chem Soc. 2003 Apr 1;125(15):4430–1.
31. Zhang Y, Ram MK, Stefanakos EK, Goswami DY. Synthesis, Characterization, and Applications of ZnO Nanowires. Journal of Nanomaterials. 2012;2012:1–22.
32. Ekem N, Korkmaz S, Pat S, Balbag MZ, Cetin EN, Ozmumcu M. Some physical properties of ZnO thin films prepared by RF sputtering technique. International Journal of Hydrogen Energy. 2009 Jun;34(12):5218–22.
33. Rashid J, Barakat MA, Salah N, Habib SS. ZnO-nanoparticles thin films synthesized by RF sputtering for photocatalytic degradation of 2-chlorophenol in synthetic wastewater. Journal of Industrial and Engineering Chemistry. 2015 Mar;23:134–9.
34. Kołodziejczak-Radzimska A, Jesionowski T. Zinc Oxide—From Synthesis to Application: A Review. Materials. 2014 Apr 9;7(4):2833–81.
35. Hong R, Pan T, Qian J, Li H. Synthesis and surface modification of ZnO nanoparticles. Chemical Engineering Journal. 2006 Jun;119(2–3):71–81.
36. Li X, He G, Xiao G, Liu H, Wang M. Synthesis and morphology control of ZnO nanostructures in microemulsions. Journal of Colloid and Interface Science. 2009 May;333(2):465–73.
37. Pan ZW, Dai ZR, Wang ZL. Nanobelts of Semiconducting Oxides. Science (1979). 2001 Mar 9;291(5510):1947–9.
38. Kołodziejczak-Radzimska A, Jesionowski T. Zinc Oxide—From Synthesis to Application: A Review. Materials. 2014 Apr 9;7(4):2833–81.
39. Flores-Carrasco G, Carrillo-López J, Luna-López JA, Martínez-Martínez R, Espinosa-Torres ND, Rabanal ME. Structural and Morphological Properties of Nanostructured ZnO Particles Grown by Ultrasonic Spray Pyrolysis Method with Horizontal Furnace. Advances in Materials Science and Engineering. 2014;2014:1–6.
40. Karnati P, Haque A, Taufique M, Ghosh K. A Systematic Study on the Structural and Optical Properties of Vertically Aligned Zinc Oxide Nanorods Grown by High Pressure Assisted Pulsed Laser Deposition Technique. Nanomaterials. 2018 Jan 25;8(2):62.

41. ElZein B, Yao Y, Barham AS, Dogheche E, Jabbour GE. Toward the Growth of Self-Catalyzed ZnO Nanowires Perpendicular to the Surface of Silicon and Glass Substrates, by Pulsed Laser Deposition. Materials. 2020 Oct 5;13(19):4427.
42. Bellardita M, di Paola A, Yurdakal S, Palmisano L. Preparation of Catalysts and Photocatalysts Used for Similar Processes. In: Heterogeneous Photocatalysis. Elsevier; 2019. p. 25–56.
43. Cheng AJ, Tzeng Y, Zhou Y, Park M, Wu T hsueh, Shannon C, et al. Thermal chemical vapor deposition growth of zinc oxide nanostructures for dye-sensitized solar cell fabrication. Applied Physics Letters. 2008 Mar 3;92(9):092113.
44. Xiang B, Wang P, Zhang X, Dayeh ShadiA, Aplin DPR, Soci C, et al. Rational Synthesis of p-Type Zinc Oxide Nanowire Arrays Using Simple Chemical Vapor Deposition. Nano Letters. 2007 Feb 1;7(2):323–8.
45. Hargittai I. Christopher Hammond: The basics of crystallography and diffraction. Third edition. Structural Chemistry. 2009 Aug 19;20(4):751–751.
46. Deenathayalan J, Saroja M, Venkatachalam M, Gowthaman P, Muthukumarasamy N, Senthil TS, et al. Optical and Structural Properties of ZnO Nanorods Prepared by Chemical Bath Deposition Method. Advanced Materials Research. 2013 Mar;678:207–11.
47. Somvanshi D, Jit S. Analysis of Temperature-Dependent Electrical Characteristics of n-ZnO Nanowires (NWs)/p-Si Heterojunction Diodes. IEEE Transactions on Nanotechnology. 2014 Jan;13(1):62–9.
48. Jurablu S, Farahmandjou M, Firoozabadi TP. Sol-gel synthesis of zinc oxide (ZnO) nanoparticles: Study of structural and optical properties. Journal of Sciences, Islamic Republic of Iran. 2015;26(3).
49. Smith KCA, Oatley CW. The scanning electron microscope and its fields of application. British Journal of Applied Physics. 1955;6(11).
50. ’Jonathan A. How scanning electron microscopes work . http://science. howstuffworks. com/scanning-electronmicroscope2. htm. 2009.
51. Sutton MA, Li N, Joy DC, Reynolds AP, Li X. Scanning electron microscopy for quantitative small and large deformation measurements Part I: SEM imaging at magnifications from 200 to 10,000. Experimental Mechanics. 2007;47(6).
52. Nguyen VC, Kim J, Dang PT, Zumuukhorol M, Cuong TV, Hong CH, et al. Application of a ZnO nanorod layer to display retarder: dependence of the optical property on synthesis conditions. Optical Materials Express. 2020 Dec 1;10(12):3315.
53. Farhat OF, Halim MM, Abdullah MJ, Ali MKM, Allam NK. Morphological and structural characterization of single-crystal ZnO nanorod arrays on flexible and non-flexible substrates. Beilstein Journal of Nanotechnology. 2015 Mar 12;6:720–5.
54. Torres-Rivero K, Bastos-Arrieta J, Fiol N, Florido A. Metal and metal oxide nanoparticles: An integrated perspective of the green synthesis methods by natural products and waste valorization: applications and challenges. InComprehensive Analytical Chemistry 2021 Jan 1 (Vol. 94, pp. 433-469). Elsevier.
55. Yang X, Hu J, He J. Effect of interfacial charge relaxation on conducting behavior of ZnO varistors under time varying electric fields. Applied Physics Letters. 2017 May;110(18):182104.
56. Parvez Ahmad MD, Venkateswara Rao A, Suresh Babu K, Narsinga Rao G. Particle size effect on the dielectric properties of ZnO nanoparticles. Materials Chemistry and Physics. 2019;224.
57. Badali Y, Altındal Ş, Uslu İ. Dielectric properties, electrical modulus and current transport mechanisms of Au/ZnO/n-Si structures. Progress in Natural Science: Materials International. 2018 Jun;28(3):325–31.
58. Jebli M, Rayssi Ch, Hamdaoui N, Rabaoui S, Dhahri J, ben Henda M, et al. Effect of Nb-doping on the structural and electrical properties of Ba0.97La0.02Ti1-xNb4x/5O3 ceramics at room temperature synthesized by molten-salt method. Journal of Alloys and Compounds. 2019 May;784:204–12.
59. Saadi H, Benzarti Z, Rhouma FIH, Sanguino P, Guermazi S, Khirouni K, et al. Enhancing the electrical and dielectric properties of ZnO nanoparticles through Fe doping for electric storage applications. Journal of Materials Science: Materials in Electronics. 2021;32(2).
60. Al-Khafaji A, Soylu-Koc N, Altintas SP, Dogruer M, Altug C, Gokcen M, et al. Investigation of frequency-dependent dielectric properties of ZnO nanorods grown on Si

wafer: In/ZnO/p-Si heterostructure. Journal of Materials Science: Materials in Electronics. 2022;33(10).